Development of Chemical Probes for the Lysine Acetyltransferases and Discovery of Lysine Isobutyrylation

by

ZHESI ZHU

(Under the Direction of Y. George Zheng)

ABSTRACT

Post-translational modifications of histones are critical to a plethora of cellular processes. A key histone modification, histone lysine acetylation, is well orchestrated by histone acetyltransferases (HATs) and histone deacetylases (HDACs). HATs function as epigenetic writers by transferring an acetyl group from acetyl-coenzyme A (Ac-CoA) to the ε-amino groups of lysine residues to form ε-N-acetyllysine in a histone or non-histone substrate. Despite the intricate regulation, HAT overexpression has been correlated with disease states, such as cancer and inflammatory diseases. HAT inhibitors, therefore, are emerging as promising therapeutics to tune histone acetylation. In this work, we examined structure-activity relationships between acyl-CoAs and HATs and observed correlation between acyl chain length and inhibitory potency. Based on our findings, we synthesized several CoA derivatives, and evaluated their biological activities *in vitro* and in cells. In particular, a dimethylaminonaphthalene-CoA derivative A433-CoA was found to be one of the most potent inhibitors for the HAT p300. This selective HAT inhibitor will be a useful biological tool to investigate the role of p300-related pathways and may serve as a

lead for development of novel anti-neoplastic therapeutics. In addition, we identified a novel histone modification, lysine isobutyrylation, which gains more in-depth knowledge of lysine acylations especially lysine butyrylation. We also found that both butyrate and isobutyrate could inhibit HDAC activity, increase levels of histone acetylation and therefore influence global gene transcription. We hope that our work can shed light on PTMs and epigenetics, providing clues for studies in epigenetics.

INDEX WORDS: Histone acetyltransferases (HATs), lysine acetyltransferases (KATs), post-translational modifications, histone acylations, acyl-CoAs, lysine isobutyrylation, chemical probes

Development of Chemical Probes for the Lysine Acetyltransferases and Discovery of Lysine Isobutyrylation

by

ZHESI ZHU

B.S., China Pharmaceutical University, China, 2013

MSc, University of Edinburgh, U.K., 2014

A Dissertation Submitted to the Graduate Faculty of The University of Georgia in Partial Fulfillment of the Requirements for the Degree

DOCTOR OF PHILOSOPHY

ATHENS, GEORGIA

2021

Development of Chemical Probes for the Lysine Acetyltransferases and Discovery of Lysine Isobutyrylation

by

ZHESI ZHU

Major Professor:	Y. George Zheng
Committee:	Shelley Hooks
	Arthur Roberts
	May Xiong
	Vladimir Popik

Electronic Version Approved:

Ron Walcott
Dean of the Graduate School
The University of Georgia
May 2021

ACKNOWLEDGEMENTS

I would like to thank my advisor, Dr. Y. George Zheng, who is an excellent scientist that continues to pursue the mechanism of phenomena and support curiosity. I am grateful for his mentoring, patience, and perseverance. I am also grateful for my graduate advisory committee, Dr. May Xiong, Dr. Arthur Roberts, Dr. Vladimir Popik, and Dr. Shelley Hooks, for their support and constructive feedback.

I want to thank our former post docs Dr. Jing Zhang and Dr. Maomao He for their expertise in synthesis. I am also thankful for the fun and supportive Zheng lab members Mr. Tyler Brown, Mr. Jiabao Song, Ms. Mengtong Cao and Ms. Tran Dang. I would like to thank Dr. Zhen Han and Dr. Liza Ngo for training me in recombinant protein expression and making contribution to my project.

Also, I want to especially thank my family for their enduring support and love.

Table of Contents

CHAPTER 1 INTRODUCTION AND LITERATURE REVIEW

1.1 Chromatin and epigenetic modifications

Chromatin is a complex of macromolecules composed of DNA and proteins, which is found inside the nucleus of eukaryotic cells[1]. The primary protein components of chromatin are histones that help organize DNA into "bead-like" structures called nucleosomes by providing a base on which the DNA can be wrapped around. A nucleosome consists of 147 base pairs of DNA strands that are wrapped around a set of 8 histones called an octamer consisting of two copies of core histones H3, H4, H2A and H2B[2]. Nucleosomes are linked by H1 protein to create highly compressed structures named chromatin fibers which are further coiled and condensed to form chromosomes[3]. Chromatin makes it possible for a number of cell processes to occur including DNA replication, transcription, DNA repair, and cell division[4].

Epigenetics is the study of heritable phenotype changes that do not involve alterations in the DNA sequence add ref. At least three systems including DNA methylation, histone modifications and non-coding RNA (ncRNA)-associated gene silencing are currently considered to initiate and sustain epigenetic changes[5]. As an important component of protein post-translational modifications (PTMs), histone modifications are key epigenetic regulators that control chromatin structure and gene transcription, thereby impacting on various cellular phenotypes and processes add ref. There are three modifiers in histone modifications: writers, readers and erasers add ref. While writers are enzymes that add certain chemical groups to unmodified histone, erasers

are the ones that remove chemical groups from the modified histones. Readers do not add or remove chemical groups, but recognize these histone modification marks to produce functional outcomes. By establishing different combinations of histone PTMs, histone modifiers can form the diverse "histone codes" that can recruit other proteins to form transcriptional complex, in addition to stabilizing or destabilizing the chromatin structure. Some of the major modifiers and functions are listed in **Table 1.1.**

Table 1 Histone modifications, modifiers and functions

Histone Modifications	Modifiers	Functions
Methylation	PRMTs[6], EZH1/2[7]	Transcriptional activation or repression
Acetylation	HATs[8], HDACs[9]	Transcriptional activation or repression DNA repair
Phosphorylation	Aurora B[10], MSK[11]	Mitosis, meiosis, transcriptional activation
Ubiquitylation	USPs[12]	Transcriptional activation, DNA damage response
SUMOylation	SAE1/SAE2[13]	Transcriptional repression

1.2. Histone acetylation and deacetylation

Histone acetylation and deacetylation are reversible processes by which the ε-amino group of lysine residues within the N-terminal tail are acetylated and deacetylated as part of gene regulation (**Figure 1.1**). In physiological conditions, the cationic ε-amino group interacts with anionic phosphate groups on DNA molecules by electrostatic forces, which in turn controls the chromatin architecture. By neutralizing or reinforcing the charges on lysine, histone acetylation and deacetylation alter the binding forces between DNA strands and histone, loosen or tighten the chromatin structure, leading to transcriptional activation or inactivation.

Histone acetylation is one of the best-studied histone modifications. As acetylated lysines on chromatin can promote open chromatin by being bound by a variety of

transcription factors, its deregulation can lead to aberrant gene expression and epigenetic malignancy, especially cancer[14]. Acetylation also occurs on a broad range of non-histone proteins including tumor suppressors and oncogenes, such as p53 and c-myc to regulate protein stability, DNA binding, protein-protein interaction, enzymatic activity[15]. On the other hand, hypoacetylation caused by overexpression of HDACs has been found in a panel of different cancers and correlates with poor patient prognosis, making it a compelling therapeutic target for cancer treatment[16]. Indeed, HDAC inhibitors are research hotspots and well-developed epigenetic drugs. Vorinostat and romidepsin are FDA-approved HDAC inhibitors for the treatment of refractory cutaneous T cell lymphoma (CTCL), and many others are currently under different stages of clinical assessment[17].

Despite the huge progress targeting HDACs in the clinic, targeting HATs has been challenging and development of HAT inhibitors has been lagged behind. C646[18], A-485[19] and B026[20] are relatively potent and selective synthetic inhibitors for p300/CBP based on the virtual screening using a p300/Lys-CoA crystal structure (PDB code: 3BIY).[21] Their efficacy in preclinical models warrant more in-depth studies. HAT inhibitors targeting other HATs are also being developed, mostly peptide-based bisubstrate inhibitors which, however, lack cell permeability.[22,23] Therefore, their cellular applications have been limited.

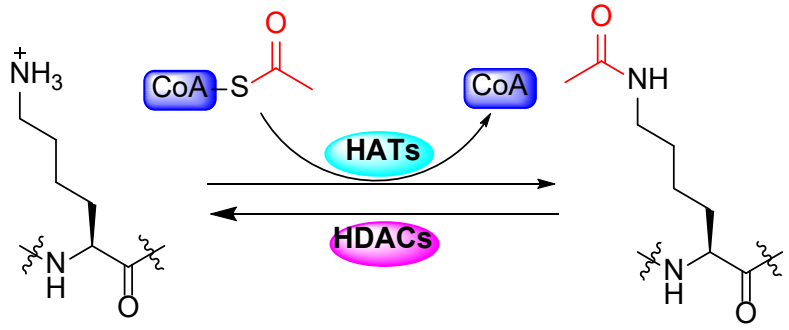

Figure 1.1 Histone acetylation and deacetylation. These two modifications are reversibly catalyzed by HATs and HDACs, using acetyl-CoA as the acetyl group donor.

1.3. Histone acetyltransferases (HATs)

Histone acetyltransferases (HATs) are enzymes that catalyze the acetylation of lysine amino acids on histone proteins by transferring an acetyl group from acetyl-CoA to form ε-N-acetyllysine[24]. Based on their subcellular localization, HATs are usually divided into two different classes. Whereas type A HATs are located in the nucleus and are involved in the regulation of gene expression through acetylating nucleosomal histones, type B HATs are located in the cytoplasm and responsible for acetylating newly synthesized histones prior to their assembly into nucleosomes[25]. So far at least four families of HATs have been identified including MYST (named after the founding members MOZ, ySAS3, ySas2 and Tip60), PCAF/GCN5, p300/CBP, and others such as better specify "others" [24]. MYST family HATs utilize a "ping-pong" mechanism involving the formation of a covalent acetyl-cysteine intermediate (Ac-Cys) and transfer of Ac to the target Lys[26]. GNAT (Gcn5-related N-acetyltransferases) includes GCN5, PCAF, HAT1, and carry out histone acetylation using a conserved Glu for proton transfer to the target Lys[27]. p300/CBP catalyze acetylation by a "hit and run" mechanism or Theorell–Chance theory[28]. Their catalytic activity is regulated by interaction with other cofactors and autoacetylation[28].

1.4 Histone acetyltransferases p300 and HAT1

Histone acetyltransferase p300 is encoded by the *EP300* gene. It functions as histone acetyltransferase and transcriptional co-activator that regulates transcription of genes via chromatin remodeling by disrupting the binding between histone and DNA

strands add ref. p300 and its homolog CBP are the most promiscuous HAT enzymes; they are capable of acetylating all the 4 core histones as well as at least 70 other proteins[29]. p300/CBP function primarily as transcriptional cofactors for a number of nuclear proteins add ref. They are also able to interact with the basal transcription factors TATA-binding protein (TBP) and TF_{IIB} and can form a complex with RNA polymerase II[30]. The molecular function of p300/CBP in human diseases is, however, enigmatic and complicated. On one hand, they are cofactors for oncoproteins transforming viral proteins (e.g., E1A) and on the other, they can bind to tumor suppressor proteins (e.g., p53, E2F, Rb, or BRCA1).[30]

Histone acetyltransferase HAT1 is the founding member of HATs. Originally, HAT1 was identified as a cytosolic HAT that acetylates newly synthesized histone H4 before their deposition in replicating chromatin ref. *In vitro*, HAT1 acetylates Lys5 and Lys12 of free histone H4, and this specificity is consistent with the pattern of acetylation found on newly synthesized histone H4 *in vivo*[31]. Like p300, the function of HAT1 remains less studied despite of numerous reports regarding its role in disease development. Research has shown that HAT1 was overexpressed in liver cancer[32] and pancreatic cancer[33], indicative its potential as a target of anticancer drug discovery.

1.5. Other histone lysine acylations and histone butyrylation

Apart from the classical lysine acetylation, other types of acylations have been discovered, including propionylation (Kpro)[34], butyrylation (Kbu)[34], 2-hydroxyisobutyrylation (Khib)[35], succinylation (Ksucc)[36], malonylation (Kma)[36], glutarylation (Kglu)[37], crotonylation (Kcr)[38] and β-hydroxybutyrylation (Kbhb).[39] These acylations are involved in fatty acid metabolism or ketone body metabolism, with acyl-

CoAs as acyl donors that may generated from different metabolic pathways.[40] For example, glutaryl-CoA is an important intermediate in lysine and tryptophan metabolism.[37] Whereas propionyl- and succinyl-CoA participate in metabolism of odd-numbered fatty acids[34], malonyl-CoA participates in fatty acid and polyketide biosynthesis[36].

Among these acylations, lysine butyrylation (Kbu) has drawn remarkable attention due to study on butyrate and amino acid metabolism. It was first discovered by Zhao and coworkers as a normal straight chain n-butyrylation (Knbu) which is biochemically dependent on n-butyryl-CoA, which is metabolic intermediate from the fatty acid oxidation pathway and therefore, serving as an ample donor source for Knbu.[34] Butyrylation competes with acetylation on H4K5/K8 and prevents the binding of the reader protein Brdt on these loci, which causes delayed histone removal and gene expression in spermatogenic cells.[41] p300/CBP is known to butyrylate tumor suppressor p53[34], but it is not completely clear how butyrylated p53 would influence molecular mechanism of cancer.

1.6 Butyrate and isobutyrate

Short-chain fatty acids (SCFAs) are organic fatty acids with less than 6 carbons. They are produced within the intestinal lumen by microbial fermentation of undigested carbohydrates, and to a lesser extent, dietary and endogenous proteins entering the colon[42]. Acetate, propionate, and butyrate are the most abundant in the gastrointestinal tract (GIT). Butyric acid or butyrate is formed in the human colon by microbial fermentation of carbohydrates.[43] Isobutyrate can also be taken in by food or environment, or produced by gut microbes. Studies have demonstrated that n-butyrate is an HDAC inhibitor that inhibits growth cancer cells[44,45], but it is not completely understood whether isobutyrate could also

be HDAC inhibitors. Efforts to exploit the potential of butyrate in clinical application of cancer treatment are disappointing due to its poor pharmacological properties (short half-life and first-pass hepatic clearance) and multiple doses needed to achieve therapeutic concentrations *in vivo*.

1.7 Rationale and Goal for this Work

As reviewed in this chapter, lysine acetylation is important for regulating gene transcription, DNA damage and cell signaling[46]. This PTM is regulated by several families of HATs that are upcoming targets in drug discovery with potential applications in many diseases especially cancer[47]. Nevertheless, developing HAT modulators becomes more challenging as HATs have various cellular substrates ranging from histones and transcription factors to enzymes and nuclear receptors. In addition, HATs operate as part of multi-protein complexes which determine their functions, their enzymatic activities and their substrate specificities in physiological conditions[47]. This complicates translational research on recombinant enzymes to cellular studies and *in vivo* studies. Many HAT inhibitors have been identified with micro- or submicro levelled potency[48], but most of them suffer from undesired properties such as poor cell permeability, complexity of cellular environment, or lack of selectivity between HAT subtypes and other enzymes. [49] In addition, presence of other proteins can modulate HAT activity by the formation of protein–protein complexes which also affect the catalytic mechanism as well as efficiency of HATs.[48]

HATs also play a role in other types of acylations including lysine n-butyrylation with butyric acid as direct source.[34] However, branched lysine acylations have been less

studied than linear lysine acylations. Lysine acylations usually utilize acyl-CoAs as cofactor which are important intermediates in fatty and amino acid metabolism, and these modifications, usually regulated by HATs, are also involved in gene transcription and disease progression.[40]

In this work, we first studied the structure-activity relationship between acyl-CoAs and HATs, and then develop novel probes to target lysine acetylation and finally identify new histone marks. The catalytic mechanism, by which these substrates are converted by HATs, is influenced by the enzyme length and the experimental methods applied to measure the enzyme activity. These studies broaden knowledge of histone acylations. Despite the difficulty of investigating knowledge on developing HAT probes deciphering functions of HATs, state-of-the-art technology such as HPLC-MS/MS and biorthogonal labeling[50] will greatly enhance discovery of HAT inhibitors and improve their chances to become therapeutic agents.

CHAPTER 2

INHIBITORY EFFECTS OF ACYL-COAS ON HATS

2.1 Introduction

Lysine acetylation of core histones in eukaryotic chromatin is catalyzed by HATs which regulate nucleosomal remodeling and lead to chromatin structural relaxation and thereafter gene activation[46]. HATs comprise of several distinct families based on sequence and structural homology, including MYST family, GCN5/PCAF, p300/CBP and others[49]. HATs are essential to regulate gene transcription in normal cellular processes, but deregulation of HATs has also been observed in a diversity of pathological states, especially cancer[51]. As such, development of HAT modulators possesses pharmacological and therapeutical values in targeting the disease types that are caused by HAT malfunction, primarily HAT overexpression. In recent years, HAT inhibitors have been developed by various strategies. Among them are natural HAT inhibitors such as anacardic acid and curcumin which show remarkable inhibitory potency yet poor selectivity[14]. In reality, the endogenous metabolite CoA has also been found to inhibit HAT activity[52], which inspires us to gain insight into inhibition pattern of other CoA analogs and investigate structure-activity relationship between HATs and different acyl-CoAs.

Fatty acyl-CoAs are fatty acid derivatives formed of one fatty acid and one CoA molecule, joined by thioester linkage (R-CO-SCoA) to the -SH group of CoA, where R is a fatty carbon chain. Acyl-CoAs are classified according to the length of fatty acid moiety as short-chain (acetate, propionate, butyrate, i.e., C2-C4 fatty acids), median-chain (C6-

C12), long-chain (C12-C20) and very long-chain (> C20)[53]. They are important metabolic intermediates in fatty acid oxidation and amino acid catabolism. While acetyl-CoA is the classic cofactor for histone and non-histone acetylation, other acyl-CoAs have been found to be cofactors in such acylations as lysine propionylation[34], butyrylation[34], succinylation[54], etc., catalyzed by certain HATs. The crystal structures of acyl-CoAs bound to HATs have shown that those acyl-CoAs share the same binding pocket with acetyl-CoA. Therefore, it is of great interest to investigate how they would influence lysine acetylation. Herein, we present our work on profiling inhibitory patterns of CoA analogs in various HATs, providing strategies for developing CoA-based chemical tools for the mechanistic study of the HATs and pharmacological intervention.

2.2 Materials and Methods

2.2.1 Chemical Reagents

The N-α-Fmoc-protected amino acids were purchased from either Novabiochem or ChemPep Inc. High-performance liquid chromatography (HPLC) grade acetonitrile was purchased from either Sigma-Aldrich. Phenylmethanesulfonyl fluoride (PMSF) was purchased from either Gold Biotechnology or Sigma-Aldrich. Kanamycin, ampicillin, and isopropyl β-D-1-thiogalactopyranoside (IPTG) were purchased from Gold Biotechnology. Unless otherwise stated, the remaining chemical reagents described were purchased from Thermo Fisher Scientific, Acros Organics, Sigma-Aldrich, Alfa Aesar, BDH, Research Products International Corp., Bio-Rad, or J. T. Baker.

The syntheses, purification and structural characterization of the acyl-CoA molecules used in this study were performed by Dr Maomao He.

2.2.2 Protein Expression

Full-length MOF-wild type and human GCN5 HAT domain (hGCN5-HAT)

pET19b-MOF or pET-28a(+)-GCN5 plasmid was transformed into *Escherichia coli* BL21(DE3) (Stratagene) through heat shock method. Protein expression was induced at OD_{595} 0.6-0.8 by 0.3 mM of isopropyl 1-thio-β-D-galactopyranoside (IPTG) at 16 °C overnight. Cells were harvested by centrifugation and resuspended in the lysis buffer (25 mM HEPES pH 7.0, 150 mM NaCl, 1 mM $MgSO_4$, 5% glycerol, 5% ethylene glycol and 1 mM phenylmethanesulfonyl fluoride [PMSF]). Cells were lysed on French Press and the supernatant was loaded onto the Ni-charged His-tag binding resin (Novagen) which was equilibrated with column buffer (Na-HEPES pH 7.0, 150 mM NaCl, 1mM $MgSO_4$, 10% glycerol, and 1 mM PMSF, 10% glycerol and 30 mM imidazole). Resins were washed thoroughly with column buffer, followed by washing buffer (25 mM Na-HEPES pH 7.0, 300 mM NaCl, 1 mM PMSF, 10% glycerol and 70 mM imidazole), and protein was eluted with elution buffer (25 mM Na-HEPES pH 7.0, 300 mM NaCl, 1 mM PMSF, 100 mM EDTA, 10% glycerol and 200 mM imidazole). Proteins were dialyzed against dialysis buffer, followed by concentration using Millipore centrifugal filters. Different eluent fractions were checked by 12% SDS-PAGE, and enzyme concentrations were determined by Bradford assay. Enzymes were aliquoted, flash-frozen in liquid nitrogen and stored at -80 °C for future use.

p300 HAT domain (p300-HAT)

The expression of p300-HAT (residues 1287–1666) was done following the method developed by Cole's lab[55]. pTYB2-p300 plasmid was transformed into *E.coli* BL21(DE3)

codon plus RIL strain (Stratagene) through heat shock method spreading on plates containing both ampicillin and chloramphenicol antibiotics. Colonies were harvested, grown at 37 °C in 8 mL, and inoculated to 1 L culture of 2XYT media containing both ampicillin and chloramphenicol. Protein expression was induced with 1 mM IPTG and shaken for 16 h at 16°C. The cells were collected by centrifugation at 4,000 rpm for 25 min and were resuspended in lysis buffer containing 25mM Na-HEPES pH 8.0, 500 mM NaCl, 1mM $MgSO_4$, 10% glycerol, and 2 mM PMSF.

Cells were lysed on French Press. The supernatant was purified on chitin resins equilibrated with column buffer (25mM Na-HEPES pH 8.0, 250 mM NaCl, 1mM EDTA, 0.1%Triton X-100, and 1 mM PMSF). The protein-loaded beads were thoroughly washed with the column buffer and wash buffer (25mM Na-HEPES pH 8.0, 500 mM NaCl, 1mM EDTA, 0.1% Triton X-100, and 1 mM PMSF). Next, the catalytic motif CT14 peptide (NH_2-CMLVELHTQSQDRF) was dissolved in the cleavage buffer (25mM Na-HEPES pH 8.0, 250mM NaCl, 1mM EDTA, and 200 mM 2-mercaptoethanesulfonic acid [MESNA]) and added to the column. The column was shaken at room temperature for 16 h before the protein was eluted from the column, and several volumes of cleavage buffer were added to ensure the complete protein elution. Further purification was done using the Bio-Rad NGC fast protein liquid chromatography system. p300-HAT domain protein band was checked by 12% SDS-PAGE. The enzyme was concentrated by Millipore centrifugal filters and the concentration was determined by Bradford assay. The protein was finally aliquoted, flash-frozen in liquid nitrogen and stored at -80 °C for future use.

HAT1 domain

pET28a-LIC-HAT1 plasmid was transformed into *E. coli* BL21 (DE3) codon plus

RIL strain (Stratagene) through heat shock method spreading on plates containing both kanamycin and chloramphenicol antibiotics. Protein expression was induced by 0.4 mM IPTG and incubated overnight at 15 °C. Harvested cells were resuspended in the lysis buffer containing 50 mM sodium phosphate buffer (pH 7.4) 250 mM NaCl, 5 mM imidazole, 5% glycerol 1 mM PMSF and 2 mM β-mercaptoethanol. Cells were lysed and the supernatant was loaded onto the Ni-charged His-tag binding resin (Novagen) which was equilibrated with column buffer (20 mM Na-HEPES pH 8.0, 150 mM NaCl, 1mM $MgSO_4$, 10% glycerol, and 1 mM PMSF, and 30 mM imidazole). Resins were washed thoroughly with washing buffer (20 mM HEPES pH 8.0, 250 mM NaCl, 1 mM PMSF, 5% glycerol and 30 mM imidazole), followed by washing buffer (20 mM HEPES pH 8.0, 250 mM NaCl, 1 mM PMSF, 5% glycerol and 50 mM imidazole), and protein was eluted with elution buffer (20 mM HEPES pH 8.0, 250 mM NaCl, 1 mM PMSF, 1 mM EDTA, 5% glycerol and 250 mM imidazole). Further purification was done using the Bio-Rad NGC fast protein liquid chromatography (FPLC) system. Protein band was checked by 12% SDS-PAGE. The enzyme was concentrated by Millipore centrifugal filters and the concentration was determined by Bradford assay. The protein was finally aliquoted, flash-frozen in liquid nitrogen and stored at -80 °C for future use.

2.2.3 Peptide Synthesis

All peptide sequences are based on the histone H3 and H4 N-terminal tail. Ac-H3(1-20) includes N-terminal tail of H3 residues 1-20 with N-terminus acetylated. Ac-H4(1-20) includes N-terminal H4 residues 1-20 with N-terminus acetylated. All peptides were synthesized on an AAPPTec Focus XC synthesizer from Wang resin (Novabiochem) with

N-*α*-Fmoc protected amino acids. Each amino acid was double coupled to the solid phase with 5 eq of amino acid/HCTU [*O*-(1*H*-6-chlorobenzotriazol-1-yl)-1,1,3,3-tetramethyluronium hexafluorophosphate] (Novabiochem and ChemPep) and 20 eq of *N*-methyl-morpholine (NMM). The Fmoc deprotection reactions were performed with 20% (v/v) piperidine in dimethylformamide (DMF). The N-terminus of each peptide was acetylated by mixing the Fmoc deprotected peptides with 50 eq acetic anhydride, 50 eq DIPEA prepared in DMF (4:1, DMF:acetic anhydride) for 30 min. Peptides were cleaved from Wang resin with 2.5% ethanedithiol (EDT), 5% deionized water, 5% thioanisole, 5% phenol, 1% triisopropylsilane, and 81.5% trifluoroacetic acid (TFA). Peptides were precipitated in cold diethyl ether and pelleted by centrifugation (5 min, 2000 rpm). After centrifugation, the crude peptides were dissolved in water for lyophilization. Purification was performed on a Shimadzu reversed-phase high-performance liquid chromatography (RP-HPLC) system equipped with a Polaris 5 C18-A, 150 mm × 21.2 mm column (Agilent). Peptides were purified with a linear gradient using 0.05% TFA in water and 0.05% TFA in acetonitrile as the two mobile phases. The purified peptides were confirmed and characterized by MALDI, and the peptide purity was checked by analytical HPLC.

2.2.4 Enzymatic HAT assay

Following the protocol developed by Zheng's lab[56], the SPA experiments were conducted in a 96-well plate (Isolate-96; Perkin Elmer) at 30°C using a reaction buffer containing 50 mM HEPES (pH 8.0) and 1 mM EDTA. The cofactor used as an acetyl donor was [^{3}H]Ac-CoA (PerkinElmer), and the substrate was either H4(1–20)-BTN or H3(1–20)-BTN. The 30 μL reaction volume typically consisted of 2.5 μM of substrate, followed by

1 μM [^{3}H]Ac-CoA. After 5 min of incubation, 0.050 μM of HATs (final concentration) were added and samples were re-incubated for 15 min. The reaction was quenched with 30 mL of 1 M guanidium HCl and 10 μL of suspended 20 mg/mL streptavidin-coated SPA beads (Perkin Elmer) in the reaction buffer were added to each well and thoroughly mixed. The plate was placed in the MicroBeta2 scintillation counter (Perkin Elmer) in total darkness for 1 min before each of the wells containing samples was scanned. Samples were performed in duplicate and were typically within 20% of each other. IC_{50} values were obtained by quantification of formed product at various concentrations of inhibitors, and fit with equation 1. Relative activity of protein in presence of the inhibitor is normalized to the value of product formation without inhibitor present.

$$\text{Relative Activity} = 1/(1+([\text{Inhibitor}]/IC_{50})^{h}$$

2.3 Results

We first examined the effects of CoA and neutral short-chain acyl-CoAs (SCACs) including propionyl-, butyryl-, isobutyryl-, and crotonyl-CoA on four HAT representatives (**Table 2.1**). As an acyl group carrier and global regulator of cellular metabolism, CoA itself can inhibit HATs to varying degrees. On MOF it possesses unremarkable potency (IC_{50}: 33.2 μM), whereas neutral short-chain acyl-CoAs show better activities with IC_{50} values ranging from 2 to 12 μM. Crotonyl-CoA, with a rigid structure, is the least active (IC_{50}: 12.1 μM) possibly due to its less flexible acyl chain that is poorly-accommodated in the binding pocket in MOF. Butyryl- and isobutyryl-CoA has similar activities against MOF, with isobutyryl-CoA being slightly potent (IC_{50}: 3.8 μM), suggesting that the branched chain may favor inhibition yet not to a great extent. On GCN5, CoA has a leading inhibitory activity over other SCACs (IC_{50}: 5.5 μM), almost as twice as that of propionyl-

CoA (IC_{50}: 10.5 μM). Isobutyryl-CoA, on the other hand, possesses almost 2-fold potency of butyryl-CoA (IC_{50}: 18.0 μM) possibly because the side-chain methyl group may restrict the rotation and enhance hydrophobic interactions between the acyl chain and the enzyme. Crotonyl-CoA is the worst SCAC inhibitor for GCN5 with IC_{50} of 46.3 μM, which may result from unsaturation that could hinder the flexibility of the side chain and make it more difficult for crotonyl-CoA to bind within the pocket.

Table 2.1 Structure-activity relationship between neutral short-chain acyl-CoAs (SCACs) and HAT representatives: MOF, GCN5, p300 and HAT1. IC_{50} values were measured by scintillation proximity activity (SPA) assay, and shown in Mean ± SD.

Compound	**Structure**	**SPA IC_{50} (μM)**			
		MOF	GCN5	p300	HAT1
Coenzyme A	CoASH	33.2 ± 4.7	5.5 ± 0.6	22.4 ± 7.1	11.1 ± 0.5
Propionyl-CoA	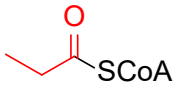	2.1 ± 0.1	10.5 ± 0.5	8.2 ± 0.9	1.7 ± 0.1
Butyryl-CoA	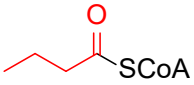	4.7 ± 0.2	35.2 ± 1.6	4.4 ± 0.2	1.1 ± 0.2
Isobutyryl-CoA	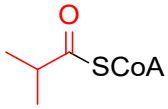	3.8 ± 0.2	18.0 ± 0.4	7.6 ± 0.2	2.4 ± 0.1
Crotonyl-CoA	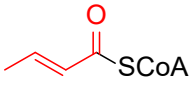	12.1 ± 1.4	46.3 ± 3.3	1.0 ± 0.1	13.7 ± 1.2

While less potent against other HATs, crotonyl-CoA outruns other SCACs against p300 (**Table 2.1**, IC_{50}: 1.0 μM). The other hydrophobic SCACs behave well against HAT1 with IC_{50} values under 3 μM. It is interesting that isobutyryl-CoA is twice potent than the

linear n-butyryl-CoA in inhibiting HAT1, which is similar with inhibition pattern for GCN5, also a member of GNAT family. Crotonyl-CoA is again the worst HAT1 inhibitor among tested SCACs (IC_{50}: 13.7 μM), almost the same as that of CoA (IC_{50}: 11.1 μM). In short summary, increased acyl chain length may favor inhibition of saturated SCACs to MOF, p300 and HAT1, whereas the less flexible crotonyl-CoA has the best potency and selectivity towards p300 with the worst potency towards GCN5. These findings demonstrate distinction among neutral SCACs caused by unsaturation and the branched structure.

We also examined the inhibitory effects of median- and long-chain acyl-CoAs (MCACs and LCACs). As shown in **Table 2.2**, hexanoyl-CoA and octanoyl-CoA have the best potency towards p300 with IC_{50} values less than 1.0 μM. While hexanoyl-CoA is not a remarkable inhibitor for HAT1 (IC_{50}: 17.2 μM), it is the most selective towards p300. In general, LCACs are excellent HAT inhibitors yet with poor selectivity. Of note, the long-chain palmitoyl-CoA and the unsaturated palmitoleoyl-CoA possess decent pan-acetylation inhibition ($IC_{50} < 1$ μM) against tested HATs. This finding is in agreement with a previous study reported by Montgomery et al[52], which suggests a close connection between epigenetics and metabolism.

Table 2.2 Structure-activity relationship between median- and long-chain acyl-CoAs (MCACs and LCACs) and HAT representatives: MOF, GCN5, p300 and HAT1. IC_{50} values were measured by scintillation proximity assay (SPA), and shown in Mean ± SD.

Compound	Structure	SPA IC_{50} (μM)			
		MOF	GCN5	p300	HAT1
Hexanoyl-CoA	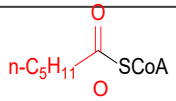	9.6 ± 0.3	2.5 ± 0.2	0.56 ± 0.04	17.2 ± 1.7
Octanoyl-CoA	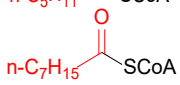	2.1 ± 0.1	0.85 ± 0.28	0.31 ± 0.01	2.2 ± 0.5
Capryl-CoA	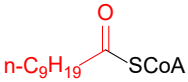	0.83 ± 0.03	0.37 ± 0.07	0.42 ± 0.04	0.54 ± 0.15
Myristoyl-CoA	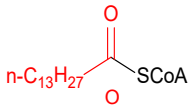	1.3 ± 0.2	0.71 ± 0.04	0.65 ± 0.05	0.93 ± 0.08
Palmitoyl-CoA	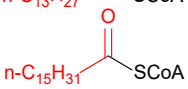	0.63 ± 0.12	0.36 ± 0.03	0.67 ± 0.04	0.75 ± 0.07
Palmitoleoyl-CoA	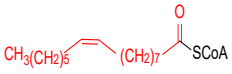	0.92 ± 0.15	0.16 ± 0.01	0.16 ± 0.03	0.51 ± 0.08

In addition to neutral acyl-CoAs, we finally examined the charge effects of C4 acyl-CoAs on HAT inhibition (**Table 2.3**). The cationic γ-butyrobetainyl-CoA has selective potency against p300 (IC_{50}: 1.3 μM) and similar potency on MOF and GCN5 (IC_{50}: 6.4 μM and 6.5 μM respectively). However, on HAT1 it has similar activity (IC_{50}: 33.13 μM) to the anionic succinyl-CoA (IC_{50}: 35.2 μM). Compared with neutral acyl-CoAs, negative charges may not assist HAT inhibition while positive charges could make contribution to inhibiting p300. Based on the observations above, we summarized correlation of IC_{50} of linear saturated acyl-CoAs and acyl chain length (**Figure 2.1**). Decrease in IC_{50} was observed in MOF, p300 and HAT1 between C0 and C3, whereas a huge increase was seen in GCN5 between C0 and C4 and a dramatic decrease to C6. The median (above C8) and long chain acyl-CoAs (above C12) are excellent HAT inhibitors with IC_{50} values below 1 μM but rather possess poor selectivity.

Table 2.3 Structure-activity relationship between different C4 acyl-CoAs and HAT representatives: MOF, GCN5, p300 and HAT1. IC_{50} values were measured by scintillation proximity activity (SPA) assay, and shown in Mean ± SD.

Compound	Structure	SPA IC_{50} (μM)			
		MOF	GCN5	p300	HAT1
Butyryl-CoA	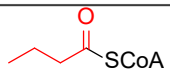	4.7 ± 0.2	35.2 ± 1.6	4.4 ± 0.2	1.1 ± 0.2
Isobutyryl-CoA	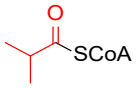	3.8 ± 0.2	18.0 ± 0.4	7.6 ± 0.2	2.4 ± 0.1
Crotonyl-CoA	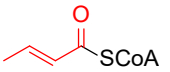	12.1 ± 1.4	46.3 ± 3.3	1.0 ± 0.1	13.7 ± 1.2
γ-butyrobetainyl-CoA	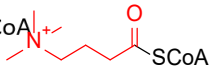	6.4 ± 0.2	6.5 ± 0.4	1.3 ± 0.1	33.6 ± 9.7
Succinyl-CoA	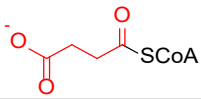	46.0 ± 4.4	25.1 ± 2.7	114.4 ± 20.3	35.2 ± 7.0

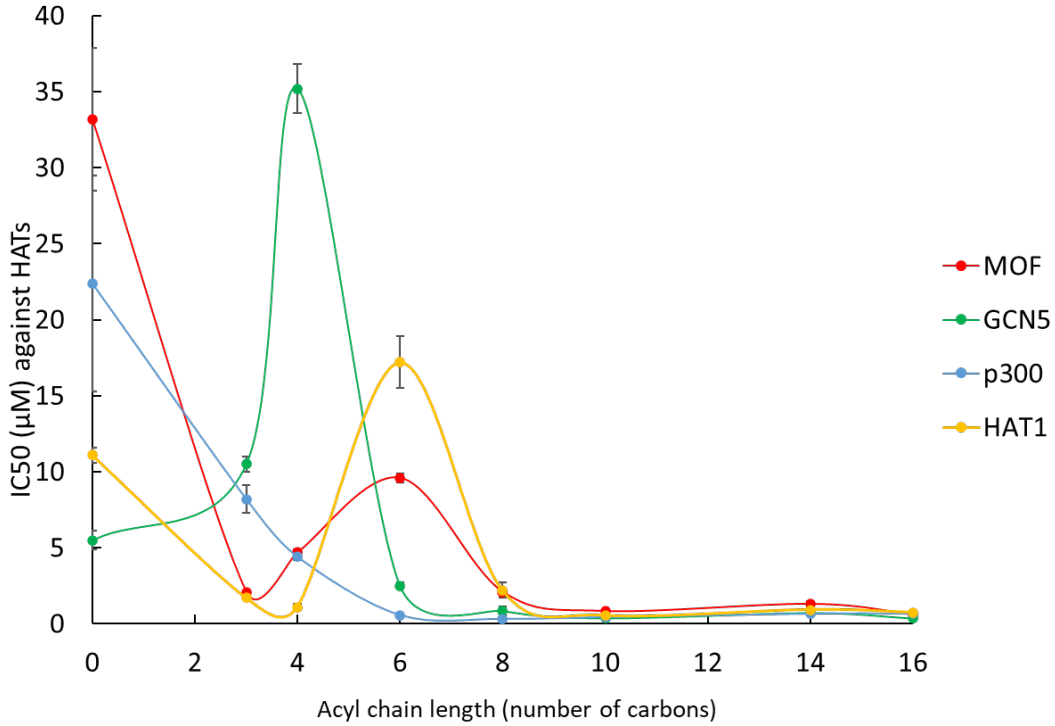

Figure 2.1 Correlation of IC_{50} values of linear saturated acyl-CoAs and acyl chain length. Acyl chain length is measured by the number of carbons in the side chain with C0 as CoA.

2.4 Discussion

Lysine acetylation of histones is an important regulatory mechanism for gene transcription that is correlated with disease progression[57]. Recent studies have shown that canonical HATs can catalyze the acylation of histones utilizing acetyl, propionyl and butyryl-CoA as cofactors.[58] However, they were reported to be less efficient in catalyzing the acylation with charged, branched or planar acyl-CoA cofactors.[59] These findings suggest that acyl-CoAs may compete with acetyl-CoA and inhibit HAT activity in structure- and charge-dependent manner. The correlation of acyl-chain and IC_{50} values (**Figure 2.1**) shows that neutral SCACs possess increased inhibitory activities on MOF, p300 and HAT1 with acyl-chain length increasing from 0 to 4, which is the opposite of GCN5 that could, however, utilize the anionic succinyl-CoA as cofactor[60]. The crystal structure of GCN5 (PDB code: 5TRL)[60] suggest that it does not have an extended aliphatic back pocket to accommodate the acyl chain, but it is of interest to investigate why hexanoyl-CoA, with 6 carbons in its acyl-chain, was shown to be better inhibitor that C4 acyl-CoAs. Hexanoyl-CoA is an ideal p300 inhibitor due to its potency as well as excellent selectivity. This may help determine the size of HAT inhibitors in designing and developing CoA-based modulators.

The results also show that crotonyl-CoA, which possesses an unsaturated moiety that seems to render its use by most HATs unfavorable except p300. Both MOF and p300 have been found to be crotonyltransferases[61,62], but crotonyl-CoA has more than 10-fold

potency in inhibiting p300 than in MOF (**Table 2.1**). The crystal structure of p300 bound with crotonyl-CoA (PDB code: 5LKZ)[63] shows that the crotonyl group was sandwiched between Trp1436 and Tyr1446, forming π-π interactions. The cationic γ-butyrobetainyl-CoA has similar potency and good selectivity towards p300 (**Table 2.3**), which suggests that π system or positive charges could greatly favor interactions between acyl-chain and the active pocket of p300. This provides an effective strategy of structural optimization for structure-based drug design. In addition to SCACs and MCACs, LCACs are found to be good pan-acetylation inhibitors. They are seemingly large molecules, but they may form micelles[64], readily occupy the binding pocket of HATs and inhibit histone acetylation in a highly efficient way. Therefore, in designing CoA-based HAT inhibitors, a long and flexible side chain may not be an optimal option for improving selectivity.

In general, we observed a strong correlation between metabolic acyl-CoAs inhibiting HAT-catalyzed acetylation with acyl-chain structures. It is thereby intriguing to design CoA-based compounds as HAT modulators or probes to explore more functions of HATs. It is also of great demand to investigate how those acyl-CoAs affect histone acetylation in cells. Such studies require improved tools for the rapid development of HAT-metabolite interactions, such as chemical proteomic approaches, which could provide novel insights into the metabolic regulation of KAT activity and strategic manipulation of acetylation-dependent signaling in disease.

CHAPTER 3

COA-DERIVATIVES AS INHIBITORS OF HISTONE ACETYLTRANSFREASE P300

3.1 Introduction

Post-translational modifications (PTMs) of histones are critical to a plethora of cellular processes including chromatin remodeling[65-67], gene transcription[68-70] and DNA repair[71-73]. A key histone modification, histone lysine acetylation, is well orchestrated by histone acetyltransferases (HATs) and histone deacetylases (HDACs). HATs function as epigenetic writers by transferring an acetyl group from acetyl-coenzyme A (AcCoA) to the ε-amino groups of lysine residues to form ε-*N*-acetyllysine in a histone or non-histone substrate such as p53, c-Myc and NF-κB[74-76]. So far at least four families of HATs have been identified including MYST (named after the founding members MOZ, ySAS3, ySas2 and Tip60), GNATs (Gcn5-related acetyltransferases), p300/CBP and SRC nuclear receptor coactivators[47]. Based on substrate specificity and subcellular localization, HATs are divided into two types[31]: type A HATs are localized in the nucleus to acetylate histones that are incorporated into chromatin, whereas type B HATs are synthesized in the cytoplasm and transported into the nucleus to acetylate newly synthesized histones H3 and H4. Whereas the therapeutic effects of HDAC inhibitors have been well characterized, less is known about potential of HATs as targets for drugs or chemical probes due largely to diverse roles of HATs in gene regulation and disease development. Despite the intricate regulation of HATs, overexpression of HATs has been recognized as a hallmark of a broad

spectrum of diseases especially cancer[57,77,78]. HAT inhibitors, are therefore emerging as promising therapeutics for cancer treatment.

Natural products and their derivatives have been shown to inhibit GNAT and p300 family members with remarkable potency yet poor selectivity[79-81]. *In vitro* studies have revealed that the endogenous CoA can inhibit various HATs via the feedback inhibition mechanism.[52,82] In recent years, bisubstrate peptide-CoA conjugates such as Lys-CoA and H3-CoA-20 have shown improved potency and selectivity[22]. Bisubstrate inhibitors and CoA derivatives have been considered as cell impermeable until a polyamine-based bisubstrate inhibitor Spd-CoA was found to inhibit HATs in cancer cells[83]. Although it did not show good selectivity and great potency to HATs[83], Spd-CoA provides evidence that CoA derivatives are able to travel through cell membrane, which inspires us to develop cell-permeable CoA-based compounds as novel HAT inhibitors. Here, we report a dimethylaminonaphthalene-CoA derivative A433-CoA as a potent and selective p300 inhibitor CoA that can also act on whole cells to inhibit histone acetylation. We aim to investigate biochemical properties of CoA derivatives and discover novel chemical probes that help dissect HAT activities.

3.2 Materials and Methods

3.2.1 Chemical Reagents

Acrylodan (6-acryloyl-2-dimethylaminonaphthalene, Cat# A433) and monobromobimane (mBBr, Cat# M1378) were purchased from Thermo Fisher Scientific. 4-bromomethyl-7-methoxycoumarin (Br-MMC, Cat# 235202). CoA (Cat# F15115) was purchased from AstaTech.

3.2.2 Protein Expression

Details are described in Chapter 2, section 2.2.2.

3.2.3 Chemical Synthesis

The syntheses and purification of these compounds were conducted by Dr. Maomao He, who was a postdoctoral research associate in Dr. Zheng's laboratory.

0.0065 mmol of CoA hydrate (5 mg) was dissolved in 1.5 mL of deionized water and cooled down on an ice bath. A433 (2.9 mg), M1378 (3.5 mg) and Br-MMC (3.5 mg, 0.013 mmol) dissolved in 1 mL of DMF respectively. The DMF solution was added dropwise to the CoA solution on ice. The reaction solution was stirred at 4 ° C overnight and then quenched by adjusting the pH to 4 with 1 M HCl. The reaction mixture was subjected to RP-HPLC purification with gradient 5—60% Acetonitrile over 30 min at a flow rate of 5 mL/min; UV detection wavelength was fixed at 214 and 254 nm. HPLC buffer was 0.05% TFA in water (solution A) and 0.05% TFA in acetonitrile (solution B). The fractions were collected and lyophilized after flash-freeze with liquid nitrogen to afford the desired products. Based on analytical HPLC the purity was 99.5%. The synthesis routes and percent yield for each reaction are shown in **Figure 3.1**.

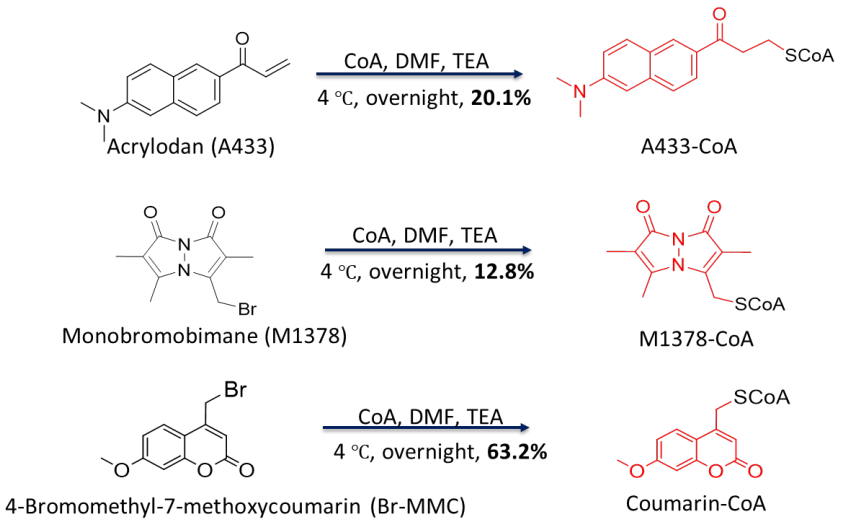

Figure 3.1 Synthesis of CoA derivatives A433-CoA, M1378-CoA and coumarin-CoA.

3.2.4. Enzymatic HAT assays

Details are described in Chapter 2, section 2.2.4.

3.2.5. Western blot analysis of histone acetylation inhibition by A433-CoA

PC-3 cells were cultured to 90% confluence in F-12K medium supplemented with 10% FBS and 1% streptomycin-penicillin antibiotics. Cells were treated with 10 μM of A433-CoA, C646 and DMSO for 24 hours, or with varied concentrations of A433-CoA for 48 hours. Total histones were extracted with EpiQuik Total Histone Extraction Kit (Epigentek, Cat# OP-0006-100) and quantified by Bradford assay. Histone extracts were then resolved on a 15% polyacrylamide gel and Kac levels were determined with Western blot using anti-acetyllysine antibody (PTM Biolabs, Cat# PTM-101). H3K18ac and H3K27ac levels were analyzed by anti-H3K18ac (Cat# 9675S) and anti-H3K27ac (Cat# 4353S) antibodies. Histone H3 was used as the loading control using histone H3 antibody (Santa Cruz Biotechnology, Cat# sc-517576).

3.2.5. Molecular docking of A433-CoA to p300

The crystal structure of p300 bound to Lys-CoA (PDB ID:3BIY) was used to perform molecular docking with the program CDOCKER built in DiscoveryStudio 4.0 (DS 4.0). The binding site of Lys-CoA was chosen as the active site with an adjusted size. The optimal binding mode was used to study ligand-receptor interactions.

3.3 Results

By means of SPA, we characterized inhibitory effects of the investigational compounds on four HAT representatives MOF, GCN5, p300 and HAT1 (**Table 3.1**). The endogenous feedback inhibitor CoA could indeed inhibit HATs, which is consistent with the literature.[52,82] Among the three synthetic CoA derivatives, A433-CoA shows a potent and selective inhibitory effect on p300 with IC_{50} of 0.37 μM, comparable to a bisubstrate p300 selective inhibitor Lys-CoA with IC_{50} of 0.32 μM which is in reasonable agreement with Cole's report[22]. It also shows moderate inhibition for MOF with IC_{50} of 8.1 μM. M1378-CoA has the worst potency against MOF, p300 and HAT1 (IC_{50} over 100 μM) and mediocre potency on GCN5 (IC_{50}: 25 μM). Another synthetic derivative coumarin-CoA exhibits similar inhibition patterns against MOF and GCN5 with IC_{50} being 11 μM and less potent activity on p300 (IC_{50}: 58 μM) and HAT1 (IC_{50}: 84 μM). All three synthetic compounds possess aromatic structures in their side chain of CoA, resulting in differentiating selectivity towards HATs. A433-CoA is also more powerful than the current p300 inhibitor C646 that has an IC_{50} of 1.6 μM.[84] Given these findings, it is of great interest to study A433-CoA as a hit and generate more S-substituted CoA derivatives for further investigations.

Table 3.1 IC_{50} values for CoA and synthetic compounds. The values written > 100 μM indicate that less than 50% inhibition was observed at the upper limit concentration of inhibitors used in the particular assay. A433-CoA shows the highest potency and selectivity against p300.

Compound	IC_{50} (μM)			
	MOF	**GCN5**	**p300**	**HAT1**
CoASH	33 ± 5	5.5 ± 0.6	22 ± 7	11 ± 1
Lys-CoA	4.9 ± 0.3	58 ± 8	0.32 ± 0.03	> 100
A433-CoA	**8.1 ± 1.8**	**19 ± 1**	**0.36 ± 0.03**	**29 ± 3**
M1378-CoA	> 100	25 ± 4	> 100	>100
Coumarin-CoA	11 ± 1	11 ± 1	58 ± 6	84 ± 10

To understand molecular basis of p300 inhibition by A433-CoA, we performed molecular docking to predict how A433-CoA interacted with p300. The putative binding mode (**Figure 3.2**) shows that the CoA moiety forms π-cation interactions with Arg1462 and Lys1456, salt bridges with Arg1410, H-bonds with Thr1411, Trp1456, Pro1439, Asp1399 and Leu1398. In particular, the dimethylaminonaphthalene group on the S-warhead is sandwiched between Tyr1397 and Trp1436, forming π-π stacking interactions with these two aromatic residues. This aromatic flank is unique to p300 binding pocket, and therefore enhancing interactions with these two aromatic residues can improve selectivity as well as potency. Hence, A433-CoA could be used as a template for structural optimization to obtain CoA derivatives with different alkyl linkers and the neighboring capping moiety.

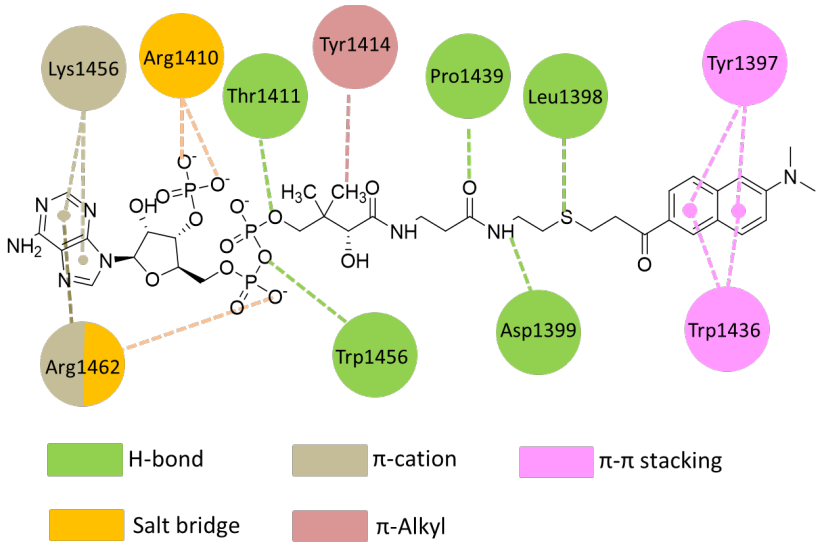

Figure 3.2 Schematic representation of molecular docking results of A433-CoA binding to p300. The crystal structure of p300 bound to Lys-CoA (PDB ID:3BIY) was used to perform molecular docking with the program CDOCKER built in DiscoveryStudio 4.0 (DS 4.0). The binding site of Lys-CoA was chosen as the active site with an adjusted size. The optimal binding mode was used to study ligand-receptor interactions. The types of interactions and engaged amino acids are indicated in respective colors. Arg1462 is shown in half orange and half brown because it is involved in two types of interactions.

We next sought for cellular inhibition of A433-CoA to prostate cancer cell line PC-3 in which p300 is overexpressed. In comparison with C646, A433-CoA did not cause significant change to histone pan-acetylation (**Figure 3.3**). This may be due to insufficient incubation time, less dosage or poor permeability. Therefore, we examined whether A433-CoA could inhibit histone acetylation, p300 targets H3K18ac and H3K27ac, in a dose-dependent manner. We observed significant decrease in levels of histone acetylation, H3K18ac and H3K27ac with increase in A433-CoA concentrations (**Figure 3.4**). Unfortunately, we were unable to observe dose-dependency in all three investigational

modifications. Nevertheless, A433-CoA, as a CoA-based compound, was shown to influence histone acetylation through direct treatment to cells. However, we only observed H3 bands (Lanes 1 and 2) in the blot. This may arise from antibody recognition or low loading amount.

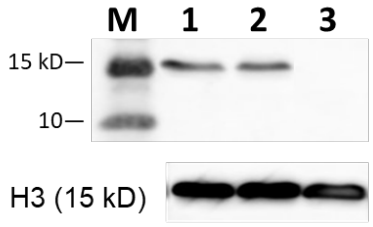

Figure 3.3 Detection of histone acetylation in PC-3 cells. PC-3 cells were treated with DMSO (Lane 1), 10 μM of A433-CoA (Lane 2) and C646 (Lane 3) for 24 hours. Total histones were extracted and tested with anti-acetyllysine antibody (PTM Biolabs, Cat# PTM-101). Histone H3 was used as the loading control.

Figure 3.4 Effects of varied concentrations of A433-CoA on histone pan-acetylation, H3K18ac and H3K27ac levels. PC-3 cells were treated with DMSO (Lane 1), varied concentrations of A433-CoA (Lanes 2-8) for 48 hours. Total histones were extracted and

analyzed with Western blot to probe for different targets. Histone H3 was used as the loading control.

3.4 Discussion

Structure-activity relationship studies of bisubstrate inhibitors indicate that CoA moiety, carbonyl group and the methylene linker are essential for strong inhibition to p300[85], and that varying S-substituents could change selectivity towards p300[86]. Despite remarkable potency and selectivity, bisubstrate inhibitors lack good cell permeability which limits their application to *in vivo* studies[22,23]. Cell-penetrating peptides have been applied for prodrug design yet with reduced potency.[87,88] Enhancing cell permeability can also be accomplished by appending nonpeptide S-substituents, as evidenced by a cell-permeable CoA-based HAT inhibitor Spd-CoA[83]. The crystal structure of p300 bound to Lys-CoA (PDB ID: 3BIY)[89] suggests that Tyr1397 and Trp1436 constitute a distinct aromatic cavity that sandwiches the S-substituent. This indicates that enhancing interactions with this cavity can potentially improve selectivity and potency. π-cation and π-π interactions are two common interactions involving aromatic systems. Enhancing π-cation interactions can be achieved by appending polyamine analogues that are widely applied in developing anti-tumor agents[90], while enhancing π-π interactions can be achieved by appending aromatic S-substituents. With a combination of synthetic chemistry, biochemical screening and structural biology, it is of great benefit to identify hits from diverse CoA derivatives that can directly applied in cell and animal cell and animal studies.

The docking model of A433-CoA to p300 (**Figure 3.2**) shows that the CoA moiety forms π-cation interactions with Arg1462 and Lys1456, salt bridges with Arg1410, H-

bonds with Thr1411, Trp1456, Pro1439, Asp1399 and Leu1398. In particular, the dimethylaminonaphthalene group on the S-warhead is sandwiched between Tyr1397 and Trp1436, forming π-π stacking interactions with these two aromatic residues. This aromatic flank is unique to p300 binding pocket, and therefore enhancing interactions with these two aromatic residues can improve selectivity as well as potency. The carbonyl group between ethylene linker and naphthalene ring is considered essential to potent p300 inhibition of bisubstrate inhibitors[86], and its absence in M1378-CoA and coumarin-CoA may explain weak inhibition of both derivatives, although the docking results do not show its interaction with p300. Moreover, the alkyl linker between the carbonyl group and CoA moiety could also influence p300 inhibition potency[85]. Although cellular results suggest that A433-CoA was less potent than C646 in inhibiting histone acetylation in PC-3 cells (**Figures 3.3 and 3.4**), it could be used as a template for structural optimization to obtain CoA derivatives with different alkyl linkers and the neighboring capping moiety, which would alter cell-permeability and influence cellular acetylation.

CHAPTER 4

IDENTIFICATION OF LYSINE ISOBUTYRYLATION AS A NEW HISTONE MODIFICATION MARK

This work is adapted with permission from the personal account article: Zhu Z, Han Z, Halabelian L, Yang X, Ding J, Zhang N, Ngo L, Song J, Zeng H, He M, Zhao Y, Arrowsmith CH, Luo M, Bartlett MG, Zheng YG. Identification of lysine isobutyrylation as a new histone modification mark. Nucleic Acids Res. 2021 Jan 11;49(1):177-189. Oxford University Press is the Publisher.

4.1 Introduction

Protein posttranslational modifications (PTMs) fundamentally impact on cellular physiology and phenotype in eukaryotic organisms.[91] Fatty acylation on the side-chain amino group of lysine residues has been recognized as an important type of reversible PTM marks that impart various regulatory functions on key cellular processes such as gene transcription, metabolism, protein homeostasis, and signal transduction.[62,92,93] So far about 20 types of lysine acylations have been discovered including acetylation (Kac), propionylation (Kpro), butyrylation (Kbu), crotonylation (Kcro), succinylation (Ksuc), malonylation (Kmal), and glutarylation (Kglu).[40,94-96] Lysine acetyltransferases (KATs) are the writer enzymes that introduce acylation marks on specific lysine residues using acyl-CoA molecules as the acyl donor.[97] Acyllysines are recognized by downstream reader proteins, and enzymatically reversed by eraser proteins, histone deacylases (HDAC).[98,99] Deregulation of lysine acylation dynamics caused by aberrant expression or mutation of either writer, reader, or eraser proteins is broadly associated with various disease phenotypes including inflammation, neurodegeneration, cancer, etc.[100-102] Even occurring on the same residues, different acylations could result in distinct biological outcomes. For instance, butyrylation competes with acetylation on H4K5/K8 and prevents the binding of the reader protein Brdt on these loci, which causes delayed histone removal and gene expression in spermatogenic cells.[41] It remains an imperative task to map out cellular substrates and modification sites of different lysine acylations and investigate their functional impacts in different physiological and pathological pathways.

In the last decade, the development of high resolution mass spectrometry has greatly facilitated discovery of many novel lysine acylation marks.[103,104] Lysine butyrylation (Kbu)

was first discovered by Zhao and coworkers as a normal straight chain n-butyrylation (Knbu) which is biochemically dependent on n-butyryl-CoA.[34] Recent studies demonstrated that KAT members p300/CBP possess lysine n-butyryltransferase activity.[105] Etiologically, n-butyryl-CoA is a metabolic intermediate from the fatty acid oxidation pathway and therefore, serving as an ample donor source for Knbu. From a chemical perspective, butyrylation mark may also exist in its isomeric structure, i.e., isobutyrylation (2-methylpropionylation) **(Figure 1)**. Our proposal is further inspired by the natural existence of isobutyryl-CoA which is endogenously generated as a result of valine catabolism and the oxidation of branched chain fatty acids.[106] Taking into account the physiological existence of isobutyryl-CoA and its structural relevance with n-butyryl-CoA, we posit that isobutyryl-CoA may also function as an acyl group donor and lead to an unexplored acylation mark in proteins, lysine isobutyrylation. Pathologically, dysregulation of isobutyryl-CoA level caused by genetic deficiency of isobutyryl-CoA dehydrogenase (IBD) is associated with multiple disease symptoms including speech delay, anemia, and dilated cardiomyopathy in newborn patients while the mechanism underlying these disorders are still poorly defined.[107,108] Hence, understanding the catabolism of isobutyryl-CoA in relationship with dynamic regulation of protein function through the PTM mechanism has a profound pathophysiological significance. In the present study, we report lysine isobutyrylation (Kibu) as a *bona fide* PTM in nuclear histones through a combined suite of biochemical, biophysical, and cellular studies.

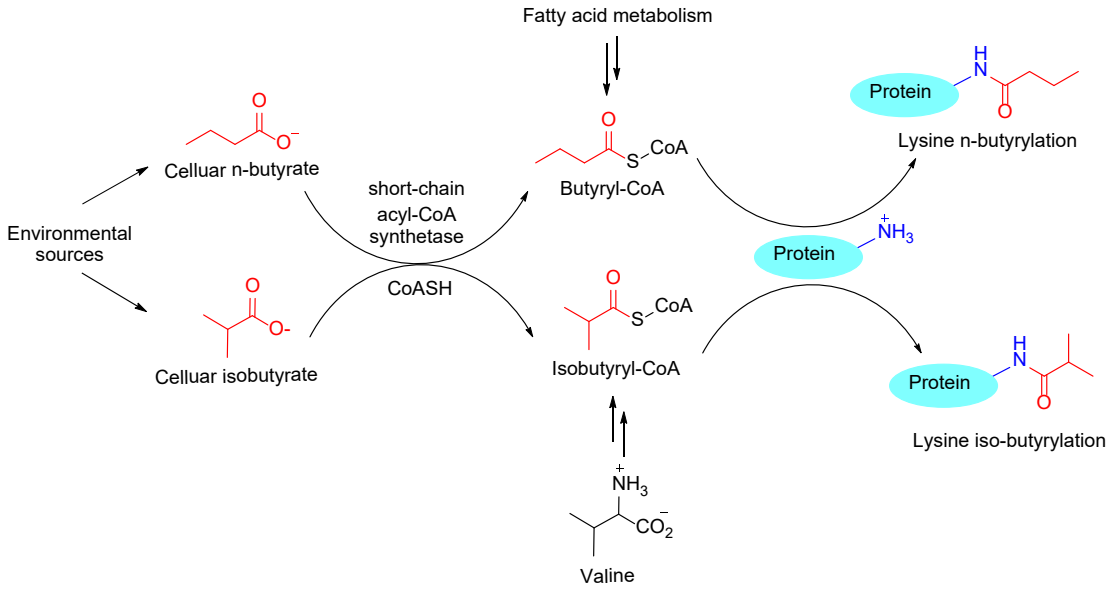

Figure 1. Distinct pathways of two isoforms of butyryl-CoA and isobutyl-CoA and their consequence in leading to protein lysine butyrylation. Lysine butyrylation was identified in 2007[34] and was recognized as n-butyrylation. In this study, we found that lysine butyrylation also exists in the form of isobutyrylation in histones. Endogenous n-butyryl-CoA is derived from fatty acid metabolism while isobutyryl-CoA is derived from valine metabolic pathway. Exogenous butyrate and isobutyrate can be converted to their acyl-CoA by the action of cellular short-chain acyl-CoA synthetases.

4.2 Materials and Methods

Quantification of butyryl-CoA level in HEK293T cells

HEK293T cells were purchased from ATCC and cultured to 90% confluence in Dulbecco's Modified Eagle Medium (DMEM) supplemented with 10% fetal bovine serum (FBS) and 1% streptomycin-penicillin. Sodium d7-isobutyrate was prepared by adding concentrated NaOH solution to d7-isobutyric acid (Sigma-Aldrich, Cat# 632007), lyophilized and quantified by reverse phase (RP)-HPLC. Cells were treated with varied

concentrations of sodium d7-isobutyrate and valine (Sigma-Aldrich, Cat#V0500) for 24 hours, and washed with ice-cold PBS buffer followed by fixing in methanol at −80 ºC for 15 minutes. Cells were collected in 50% of methanol with gentle scrape, and centrifuged at 16,000 *g* at 4 ºC. The supernatant was collected for HPLC-MS/MS analysis.

An Atlantis® T3 (4.6×150 mm, 3 μm) column with a Phenomenex SecurityGuard C-18 guard column (4.0 mm×2.0 mm) was applied to separate analytes. The column temperature was constant at 32 °C. The mobile phase A was 10 mM ammonium acetate, and mobile phase B was acetonitrile. A gradient method was applied for separation, with a 0.4 mL/min flow rate, (time/minute, % mobile phase B): (0, 6), (15, 30), (15.01, 100), (22.50, 100), (22.51, 6). The injection volume was 30 μL, and the autosampler injection needle was washed with methanol after each injection. Nitrogen was used as the desolvation gas at a flow rate of 500 L/h. The desolvation temperature was 500 °C and the source temperature was 120 °C. Argon was used as the collision gas, and the collision cell pressure was 3.5×10^{-3} mbar. Samples were analyzed in the positive ion mode. The capillary voltage was 3.2 kV, the cone voltage was 42 V and the collision energy was 22 eV. A multiple reaction monitoring (MRM) function was applied for the detection of analytes. The ion transition 838→331 was monitored for iso- and n-butyryl-CoA, and 845→338 for d7-isobutyryl CoA.

Expression and purification of p300 and HAT1

The expression of p300 HAT domain (1287-1666) was done using the semisynthetic method developed by the Cole lab.[55] A CT14 peptide aa 1653-1666 (sequence: CMLVELHTQSQDRF) was synthesized by solid-phase peptide synthesis and purified by

C18 RP-HPLC. The pTYB2 plasmid encoding the inactive p300 HAT domain (region 1287-1652) fused to intein-chitin-binding domain was transformed into *E.coli* BL21(DE3)/RIL competent cells through heat-shock method and then grown on lysogeny broth (LB)-agar plates containing both ampicillin (final concentration: 100 μg/mL) and chloramphenicol (final concentration: 50 μg/mL). Colonies were harvested and grown at 37°C in 8 mL then 1 L cultures of terrific broth media containing both ampicillin and chloramphenicol. Protein expression was induced by the addition of isopropyl β-D-1-thiogalactopyranoside (IPTG) at 1.0 mM final concentration and shaken for 16 h at 16 °C. The cells were collected by centrifugation at 4000 rpm for 25 min, suspended in lysis buffer (25 mM Na-HEPES (pH 8.0), 500 mM NaCl, 1 mM $MgSO_4$, 10 % glycerol, and 2 mM phenylmethanesulfonyl fluoride (PMSF)), and lysed by a microfluidic cell disruptor. The lysates were cleared by centrifugation to obtain the supernatant. Chitin resin were equilibrated with column buffer (25 mM Na-HEPES (pH 8.0), 250 mM NaCl, 1 mM EDTA, 0.1 % trition X-100, and 1 mM PMSF) before they were used to purify the supernatant. The column was thoroughly washed with column buffer and wash buffer (25 mM Na-HEPES (pH 8.0), 500 mM NaCl, 1 mM EDTA, 0.1 % triton X-100 and 1 mM PMSF) before being ligated to the CT14 peptide to obtain active p300. CT14 peptide was dissolved in cleavage buffer (25 mM Na-HEPES (pH 8.0), 250 mM NaCl, 1 mM EDTA, and 200 mM 2-mercaptoethanesulfonic acid (MESNA)) and added to the column. After the addition of the CT14 peptide in cleavage buffer, the column was shaken at room temperature for 16 h. The protein was then eluted from the column, and several volumes of cleavage buffer were added to ensure the complete elution. The eluted protein was further purified by cation exchange chromatography using the NGC fast protein liquid

chromatography (FPLC) system, Biorad. The identification of p300 HAT domain was confirmed using a 12 % sodium dodecyl sulfate-polyacrylamide gel electrophoresis (SDS-PAGE). Millipore centrifugal filtration was used to concentrate protein solution and the Bradford assay was used to determine final protein concentration. Lastly, the protein was aliquoted, flash frozen by liquid nitrogen and stored at -80°C.

The expression and purification of human HAT1 (20-341) was done following the method described Hong Wu et al[109]. The pET28a-LIC-HAT1 plasmid (plasmid #25239, Addgene) was transformed into BL21 (DE3)/ RIL competent cells through heat-shock and then spread on agar plates containing antibiotics kanamycin and chloramphenicol. Protein expression was induced by the addition of IPTG (final concentration: 1.0 mM) and shaken for 16 h at 16 °C. The cells were collected and suspended in lysis buffer (50 mM Na-phosphate (pH 7.4), 250 mM NaCl, 5 mM imidazole, 5 % glycerol, 2 mM β-mercaptoethanol, and 1 mM PMSF) then disrupted using the cell disruptor. The supernatant was passed through a column containing Ni-NTA resin equilibrated with column washing buffer (20 mM Tris-HCl (pH 8.0), 250 mM NaCl, 5% glycerol, 30 mM imidazole, and 1 mM PMSF) and the resin was washed with the same column washing buffer for twice. Next, the resin was washed with buffer containing a higher concentration of imidazole (20 mM Tris-HCl (pH 8.0), 250 mM NaCl, 5% glycerol, 50 mM imidazole, and 1mM PMSF) for three times. The proteins on the resin were then eluted with elution buffer (20 mM Tris-HCl (pH 8.0), 250 mM NaCl, 5% glycerol, 500 mM imidazole, and 1 mM PMSF), and dialyzed in the dialysis buffer (25 mM Tris-HCl (pH 8.0), 150 mM NaCl, 10% glycerol, 1 mM DTT) at 4°C overnight. Thrombin was added to the dialyzed protein containing HAT1 and dialyzed in thrombin cleavage buffer (20 mM Tris-HCl (pH 8.0), 100 mM NaCl, 2.5

mM $CaCl_2$, 5% glycerol, 1 mM DTT) for 20 hours at 4°C to remove the His6x-tag. The resultant protein was concentrated and purified by anion exchange chromatography using the NGC FPLC system. HAT1 purity was checked using SDS-PAGE. Millipore centrifugal filter and Bradford assay were used to concentrate and determine protein concentration, respectively. The protein was aliquoted, flash frozen by liquid nitrogen and stored at -80°C.

Synthesis of isobutyryl-CoA

2 mmol of isobutyric acid (176.2 mg) was dissolved in 5 mL of freshly distilled CH_2Cl_2. To this solution was added 1 mmol of N, N'-dicyclohexylcarbodiimide (DCC) (206.4 mg), and the reaction was allowed to proceed at room temperature for 4 h. The reaction mixture was filtered to remove dicyclohexylurea (DCU), and then CH_2Cl_2 was removed using rotary evaporation. The dried crude material was used in the next step without further purification. 0.013 mmol of CoA hydrate (10 mg) was dissolved in 1.5 mL of 0.5 M $NaHCO_3$ (pH 8.0) and cooled down on ice bath. Then the crude isobutyric anhydride (10.3 mg, 0.065 mmol) in 1 mL of CH_3CN/acetone (1:1 v/v) was added dropwise to the CoA solution. The reaction solution was stirred at 4 °C overnight and quenched by adjusting pH to 4 with 1 M HCl. The reaction mixture was subjected to RP-HPLC purification with gradient 5─45% acetonitrile over 30 min at flow rate 5 mL/min; UV detection wavelength was fixed at 214 and 254 nm. HPLC buffer was 0.05% TFA in water (solution A) and 0.05% TFA in acetonitrile (solution B). The fractions were collected, rotary evaporated and lyophilized to yield 6.34 mg white solid. The purity of final product was checked by analytical RP-HPLC and molecular weight was confirmed by MALDI MS (found $[M+H]^+$ 838.6).

Biochemical assays of lysine acyltransferase activities of KATs.

Acetyl-CoA (Sigma-Aldrich, Cat#A2181), propionyl-CoA (Chem Impex Int'l Inc, Cat# 01895) and n-butyryl-CoA (Sigma-Aldrich, Cat#B1508) salts were purchased from commercial suppliers. Synthetic histone peptides H3(1-20) or H4(1-20) (20 amino acids from the N-terminal of histone H3 and H4 (the sequence of H3(1-20) is Ac-ARTKQTARKSTGGKAPRKQL, the sequence of H4(1-20) is Ac-SGRGKGGKGLGKGGAKRHRK) were used as acyl acceptor substrates. For single-point quantification assays, 30 μM of each acyl-CoA molecule was incubated with individual KAT enzymes and 100 μM histone peptides. The enzymatic reactions were conducted in KAT reaction buffer containing 50 mM HEPES-Na and 0.1 mM EDTA-Na at pH 8.0. KAT enzymes were mixed with individual acyl-CoA molecules and peptide substrates, followed by incubation at 30 ºC for 15 minutes to allow enzymatic transfer of acyl groups to lysine substrates and release of by-product CoASH. The fluorogenic probe 7-diethylamino-3-(4'-maleimidylphenyl)-4-methylcoumarin (abbr. CPM, ThermoFisher, Cat# D346) in 100% DMSO was then added to both quench the enzymatic reaction and react with CoASH to yield the fluorescent CPM-SCoA complex for fluorescence quantification [110]. The fluorescence intensities were measured with excitation and emission wavelengths at 392 nm and 482 nm, respectively, with a FlexStation®3 microplate reader. Duplicated experiments were performed and the results were shown in a bar graph.

For kinetic characterization of p300 and HAT1 with acyl-CoA molecules, varied concentration of acyl-CoA was incubated with p300 or HAT1 and 200 μM of H4(1-20) peptide. All the reactions were conducted in the same KAT reaction buffer as the single-point assay. The fluorescence intensity was measured with the same method as the single-

point assay and catalytic rate was determined based on fluorescence intensities. Kinetic constants including binding affinity (K_m) and catalytic efficiency (k_{cat}) were determined by fitting the acyl-CoA concentration-catalytic rates to the Michaelis-Menten equation using KaleidaGraph.

Western blot analysis of HAT1 mediated *in vitro* histone H4 isobutyrylation

1 μg of human recombinant histone H4 (BioLabs, Cat# M2504S) was incubated with 50 μM n-butyryl- or isobutyryl-CoA and 0.2 μM of HAT1 at 30 ºC for 1 hour. The reaction mixture was boiled in SDS-PAGE gel loading buffer and resolved on a 15% polyacrylamide gel followed by wet membrane transfer to a nitrocellulose (NC) membrane. The NC membrane was blocked with 5% non-fat milk in Tris-Buffered Saline+0.1% Tween-20 (TBST) for 1 hour at room temperature. Anti-butyryllysine antibody (PTM BioLabs, PTM#301) at 1:2000 dilution was incubated with the membrane overnight at 4 ^{o}C. The membrane was washed with TBST buffer for three times and incubated with the goat anti-rabbit IgG-HRP (Santa Cruz Biotechnology, Cat# sc-2004) with 1:3000 dilution at room temperature for 1 hour. The membrane was then washed and subjected to chemiluminescence detection with the ECL substrate (ThermoFisher, Cat# 32209) on a LI-COR Odyssey system (LI-COR Biosciences).

Western blot analyses of *in cellulo* lysine isobutyrylation and lysine acetylation in response to isobutyrate treatment.

HEK293T cells were cultured to 90% confluence in DMEM medium supplemented with 10% FBS and 1% streptomycin-penicillin antibiotics. For in-cell Kibu level analysis, cells were treated with 10 mM d7-isobutyrate for 16 hours followed by cellular protein extraction. Whole cell lysate was extracted in M-PER™ Mammalian Protein Extraction

Reagent (ThermoFisher Scientific, Cat# 78501) with gentle sonication and core histone proteins were extracted with the EpiQuik Total Histone Extraction Kit (Epigentek, Cat# OP-0006-100). The extracted lysates and histone proteins were resolved on a 4-20% gradient gel (Biorad) and a 15% polyacrylamide gel, respectively. Kibu levels were detected by Western blot using the same procedure aforementionedFor in-cell Kac level analysis, cells were treated with 20 mM d7-isobutyrate for 24 hours followed by core histone extraction. Histone extracts were then resolved on a 15% polyacrylamide gel and Kac levels were determined with Western blot using anti-acetyllysine antibody (PTM Biolabs, Cat# PTM-101), with anti-Knbu/Kibu as the positive control using anti-butyryllysine antibody (PTM Biolabs, Cat# PTM-301) and histone H3 as the loading control using histone H3 antibody (Santa Cruz Biotechnology, Cat# sc-517576).

***In cellulo* analyses of lysine isobutyrylation in response to p300 and HAT1 overexpression.**

HEK293T cells were cultured to 90% confluence in DMEM medium supplemented with 10% FBS and 1% streptomycin-penicillin antibiotics. Plasmids N-flag-HAT1wt (GeneCopoeia, Cat# EX-I0105-M13-11) and pCMVβ-p300-myc (Addgene, Cat# 30489) were transfected into cells with Lipofectamine 3000^{TM} Transfection Reagent (ThermoFisher, Cat# L3000008). The cells were then incubated with 20 mM sodium d7-isobutyrate for 24 hours followed by core histone extraction. Kibu levels were analyzed by Western blot using the same procedure and antibodies aforementioned.

HAT1 crystallization and structural determination

HAT1 was expressed and purified as described previously.[109] HAT1 at 8 mg/mL was incubated with isobutyryl coenzyme A (IBuCoA) and histone H4 K12A mutant peptide

(amino acids 1–20 of H4) at a 1:10:5 molar ratio of HAT1:IbuCoA:H4(K12A) and crystallized using the sitting drop vapor diffusion method by mixing 2 μL of protein solution with 1 μL of the reservoir solution containing 2 M Sodium Dihydrogen Phosphate and 0.1 M MES, pH 6.5. Crystals were cryo-protected in the corresponding mother liquor supplemented with 30% glycerol and cryo-cooled in liquid nitrogen. X-ray diffraction date were collected at the Advanced Photon Source (APS) BEAMLINE 19-ID. Data were processed using XDS[111] and merged with Aimless.[112] PDB ID: 2P0W was used in Fourier transform using Refmac5.[113] Model building and visualization was performed in COOT[114] and the structure was validated with Molprobity.[115] Data collection and refinement statistics are summarized in **Table S1**. The HAT1-IbuCoA-H4(K12A) structure factors and coordinates have been deposited in the Protein Data Bank with the PDB ID: 6VO5.

HPLC/MS/MS analysis

Core histones (~4 μg) extracted from d7-sodium isobutyrate treated 293T cells were resolved in SDS-PAGE. Histones were excised from the gel, and subjected to in-gel digestion by trypsin (Tan eta al, 2011, Cell, 146: 1016-28). The digested peptide was dissolved in 2.5 μL water containing 0.1% formic acid (v/v), and then loaded onto a home-packed capillary column (10 cm length × 75 mm ID, 3 μm particle size, Dr. Maisch GmbH, Germany) which was connected to an EASY-nLC 1000 system (Thermo Fisher Scientific Inc.). The mobile phase A was water containing 0.1% formic acid (v/v), and mobile phase B was acetonitrile containing 0.1% formic acid (v/v). A 60-min gradient of 2% to 90% mobile phase B at a flow rate of 200 nl/min was used for the peptide separation. The eluted peptides were analyzed by a Q-Exactive mass spectrometer (Thermo Fisher Scientific Inc.). A Full mass scan was conducted in the Orbitrap mass analyzer in the range m/z 300 to

1,400 with a resolution of 70,000 at m/z 200. The top 15 ions were fragmented with normalized collision energy of 27 and tandem mass spectra were acquired with a mass resolution of 17,500 at m/z 200.

The obtained MS/MS spectra were searched with Mascot (Matrix Science, London, UK) against UniProt Human protein database. Mono-methylation and di-methylation on Lysine and Arginine, tri-methylation on lysine, acetylation on lysine and protein N-terminal, oxidation on methionine, and d7-isobutyrylation on lysine were specified as variable modifications. Maximum missing cleavage was set at 4, and mass tolerance was set at 10 ppm for precursor ions and ±0.05 Da for MS/MS.

RNA-seq

Total RNA was extracted using TRIzol reagent (Thermo Fisher). Indexed libraries were constructed using the Illumina TruSeq Stranded mRNA library prep kit. Samples were then sequenced on NovaSeq (PE50) with paired-end reading. Raw reads in FASTQ files were submitted for differential expression analysis using DEseq2. Gene set enrichment analysis (GSEA) was performed against KEGG pathway. Significantly altered gene sets were defined with the False Discovery Rate (FDR) and p value less than 0.25 and 0.05, respectively.

4.3 Results

Isobutyryl-CoA is an abundant metabolite in the mammalian cell

Upon its discovery with mass spectrometry, lysine butyrylation (Kbu) was defined as a straight chain n-butyrylation.[34] Nevertheless, two isomeric structures may contribute to the same molecular mass of the butyryl mark (+70 au): either normal linear butyryl or

branched isobutyryl group. Lysine acylations rely on acyl-CoA molecules as the reactive acyl group donor **(Figure 1)**; therefore, an ample pool of acyl-CoA is a prerequisite for the incidence of cognate lysine acylation. To determine cellular butyryl-CoA composition, we measured the levels of n- and iso-butyryl-CoA in human embryonic kidney 293T (HEK293T) cells with high-performance liquid chromatography tandem mass spectrometry (HPLC-MS/MS). Iso- and n-butyryl-CoA standards were resolved on the chromatogram at retention times of ~13.85 and 14.05 minutes respectively, and monitored at the same ion transition (838 → 331) on the mass spectrometer **(Figure 2A)**. The chromatographic peak area of n- or iso-butyryl-CoA molecules was integrated as the quantitation reference. Then HEK293T cell's acyl-CoA extracts were subjected to the same HPLC-MS/MS analysis and the abundance of n- and iso-butyryl-CoAs was compared. Duplicate experiments were conducted, showing that the ratios of iso- and n-butyryl-CoA were 2~3:1 **(Figure 2B)**. This data revealed that the cellular butyryl-CoA is a mixture of two isomers, both of which may act as acyl donors leading to lysine butyrylation on cellular proteins.

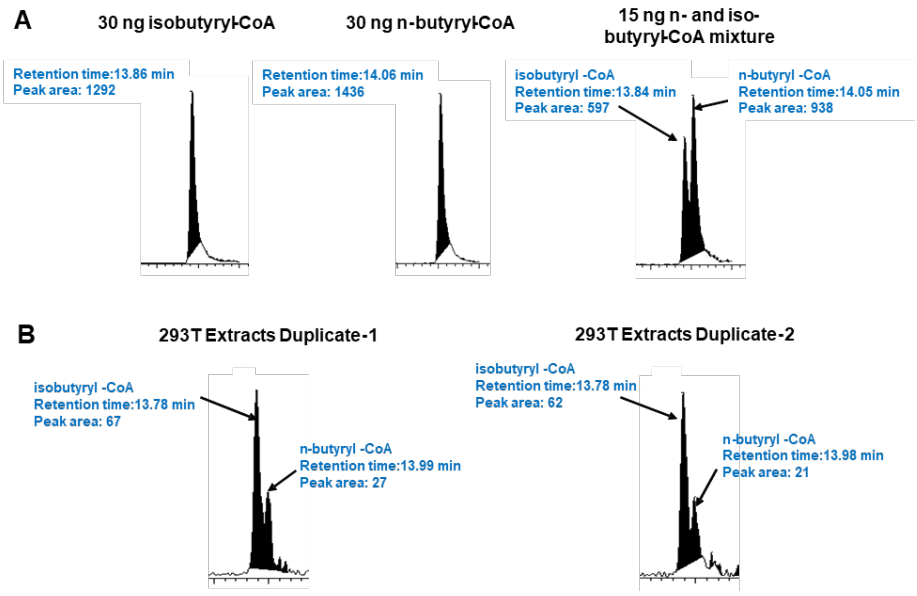

Figure 2. Detection and quantification of n- and iso-butyryl-CoA using LC-MS/MS. **A.** Control experiments showing that N- and iso-butyryl-CoA were separated with the LC-MS/MS system with the retention times at 14.06 and 13.86 minutes and were detected at the same ion transition 810 → 313. **B.** n- and iso-butyryl-CoA from the 293T cell extracts were detected under the same LC-MS/MS condition. Their levels were compared by using the integrated chromatographic peak areas.

Cellular metabolism of isobutyrate and valine lead to isobutyryl-CoA production

Acyl-CoA molecules are metabolic intermediates mostly from glucose catabolism, fatty acid β-oxidation, and amino acid degradation.[116] Also short chain fatty acids such as propionate and butyrate taken up from surrounding media can be converted to cognate acyl-CoA molecules with the catalysis of short chain acyl-CoA synthetases (ACS).[117,118] It is thus highly possible that isobutyryl-CoA can be synthesized from this pathway with isobutyrate as the source agent. Importantly, isobutyryl-CoA is a key intermediate of valine metabolism pathway so valine may also stimulate biosynthesis of isobutyryl-CoA **(Figure**

1).[119] These isobutyryl-CoA synthetic pathways would further strengthen the possibility that isobutyryl-CoA acts as an important regulator in physiological processes. Herein, we studied the effect of isobutyrate and valine treatment on the change of cellular isobutyryl-CoA level. 293T cells were treated with varied concentrations of deuterated sodium isobutyrate (d7-isobutyrate), and acyl-CoA molecules were extracted and analyzed with the HPLC-MS/MS method aforementioned. The levels of butyryl-CoA molecules were measured and normalized to total cellular proteins **(Supplementary Figure S1A)**. With the increase of d7-isobutyrate doses, d7-isobutyryl-CoA level increased drastically until a plateau was reached at 5 mM of d7-isobutyrate. The level of endogenous, non-isotopic isobutyryl-CoA remained barely changed. We also tested how isobutyryl-CoA level would change in response to valine feeding. The data showed that treatment of 293T cells with valine significantly increased the level of isobutyryl-CoA until a plateau was reached at the concentration of 5 mM valine **(Supplementary Figure S1B)**. In contrast, the level of n-butyryl-CoA was not affected by valine treatment. This observation is consistent with the aforementioned valine metabolic pathway, in which isobutyryl-CoA is an important intermediate.[119] Taken together, these data demonstrate that isobutyryl-CoA can be biosynthesized from the acyl-CoA synthetase pathway and valine metabolism, which not only defines the anabolism of isobutyryl-CoA in mammalian cells but also provides us with an amenable approach to study the dynamic change of lysine isobutyrylation levels in cellular proteins.

KAT enzymes catalyze lysine isobutyrylation

Lysine acylations are enzymatically driven by KATs, which can covalently deposit acyl groups from the cosubstrate acyl-CoA to lysine residues in protein substrates.

Identification of isobutyryl-CoA as an ample acyl-CoA donor points out the high probability for the existence of lysine isobutyrylation in cellular proteins. In this regard, it is necessary to examine whether and which KATs can catalyze this acylation reaction. We quantitatively measured the acylation activities of nine human KATs from three major KAT families, MYST, GCN5/PCAF/HAT1, and p300/CBP, using a fluorogenic assay that was designed to quantify the byproduct CoA.[110] Histone peptides H3(1-20) or H4(1-20) was used as the acyl acceptor to characterize the acetyl-, propionyl-, n-butyryl-, and isobutyrylation activities of individual KAT enzymes **(Figure S2)**. Consistent with our recent study,[120] all the tested KAT enzymes show remarkable Kpr activity, more than 20% of their nascent acetyl transfer activity, which demonstrates that almost all eukaryotic KATs may possess this intrinsic activity. Nevertheless, further increase of acyl chain length to four carbon units leads to a drastic decrease of butyrylation activity (Kbu) of KAT enzymes. Among the tested KAT enzymes, HAT1 showed outstanding isobutyrylation (Kibu) activity with ~25% of its acetylation activity, followed by HBO1 while the other KAT enzymes exhibited much lower or even barely detectable Kibu activity. p300 is known for its great cofactor promiscuity, functioning as lysine acetyl-, propionyl-, butyryl-, and crotonyltransferase.[34,62,105] Its unique acyl-CoA binding pocket enables p300 to bind with larger acyl-CoA molecules without need of protein engineering.[121,122] Therefore, we carried out steady-state kinetic characterization of p300 and HAT1 with various acyl-CoAs to determine their acyltransferase activities. The results show that the catalytic specificity constants k_{cat}/K_m of p300 with n- and isobutyrylation activities were 0.25 $min^{-1}.\mu M^{-1}$ and 0.13 $min^{-1}.\mu M^{-1}$ respectively, about 7% and 13% of p300 acetylation activity **(Figure 3)**. In comparison, Knbu and Kibu activity of HAT1 was about 13% and 31% of its acetylation

activity, respectively. Thus, both HAT1 and p300 possessed appreciable activities of lysine n-butyrylation and iso-butyrylation.

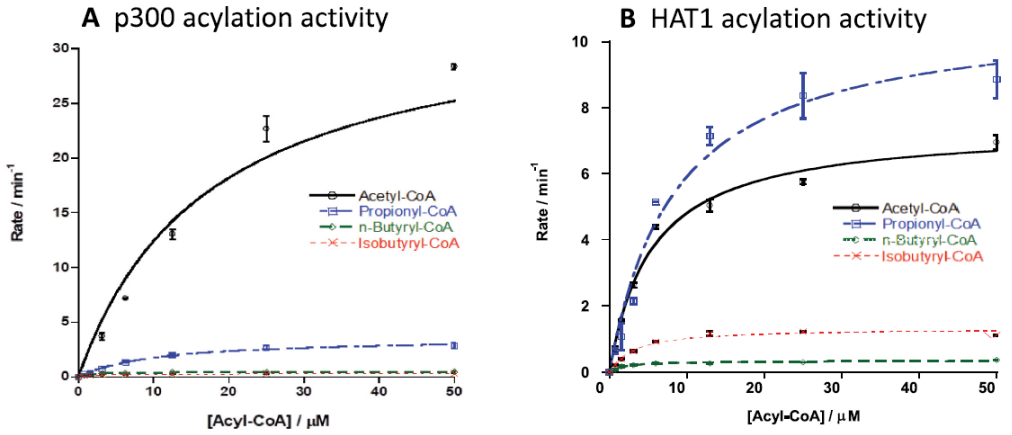

C

	Cofactor	Km (µM)	kcat (min^{-1})	kcat/Km (min^{-1}·$µM^{-1}$)
HAT1	Acetyl-CoA	5.4 ± 0.8	7.4 ± 0.3	1.4 ± 0.2
	Propionyl-CoA	8.5 ± 1.9	10.9 ± 0.8	1.3 ± 0.3
	Isobutyryl-CoA	1.9 ± 0.5	0.4 ± 0.02	0.21 ± 0.06
	Butyryl-CoA	3.1 ± 0.6	1.3 ± 0.1	0.42 ± 0.09
p300	Acetyl-CoA	17.3 ± 4.8	33.9 ± 2.9	2.0± 0.6
	Propionyl-CoA	16.3 ± 2.8	10.2 ± 0.8	0.63 ± 0.12
	Isobutyryl-CoA	2.4 ± 0.3	0.32 ± 0.01	0.13 ± 0.02
	Butyryl-CoA	1.9 ± 0.2	0.47 ± 0.01	0.25 ± 0.09

Figure 3. Kinetic characterization of p300 and HAT1 acylation activities. p300 or HAT1 was incubated with individual acyl-CoA molecule at varied concentrations and H4(1-20) peptide substrates. The enzymatic reaction was quantified using CPM assay. The reaction rate-acyl-CoA concentration were plotted with the Michaelis-Menten equation to get the kinetic constants K_m and k_{cat}. The k_{cat}/K_m value were used to evaluate lysine acylation activity. **A.** initial velocity curves of p300 with acetyl-, propionyl-, n-butyryl-, and isobutyryl-CoA. **B.** initial velocity curves of HAT1 with acetyl-, propionyl-, n-butyryl-, and isobutyryl-CoA. **C.** Kinetic parameters from the velocity data fitting. Experimental conditions: 200 μM H4(1-20) peptide, 0-50 μM acyl-CoA, 40 nM or 100 nM HAT1, 20 nM or 100 nM p300, 15 min reaction time, temperature at 30 °C.

HAT1 and p300 isobutyryltransferase activity on synthetic H3 and H4 peptides was further confirmed by MALDI-MS analysis of the reaction mixtures (**Supplementary Figure S3**). The recombinant p300 and HAT1 were incubated with isobutyryl-CoA and H3(1-20) (for p300) or H4(1-20) peptides (for HAT1) for 1 h. Next, the reaction mixture was subjected to MALDI-MS test. Product peaks (M+70) were observed in both p300 and HAT1 catalytic reactions, demonstrating that both enzymes can catalyze isobutyrylation on peptide substrates. We further tested if the isobutyrylation activity of HAT1 on histone H4 substrate can be detected with Western blot using the commercially available anti-butyryllysine antibody (PTM Biolab, Cat# PTM-301). Although this antibody was designed for detection of Knbu,[41,123] incubation of n- or iso-butyryl-CoA, histone H4 and HAT1 drastically increased the band intensity of both n-butyrylated H4 and iso-butyrylated H4, whereas lack of HAT1 induced little histone labeling (**Supplementary Figure S3**).

Hence, this anti-Knbu antibody was also able to recognize Kibu mark. Our finding on the promiscuous specificity of the anti-butyryllysine antibody indicates that some butyrylated lysines identified in previous work could be a mixture of n- and iso-butyrylated lysines. Overall, the biochemical measurements and western blot data validated the Kibu activity of HAT1 and p300. Importantly, the capability of PTM-301 antibody in recognizing Kibu mark allows for a technical means to study protein Kibu signals from the cellular contexts.

Lysine isobutyrylation is a bona fide PTM mark on nucleosomal histones

We next focused on the detection of lysine isobutyrylation (Kibu) on cellular proteins. 293T cells were treated with sodium d7-isobutyrate for 16 h, followed by extraction of the nuclear histone proteins or whole cellular proteome. The extracted proteins were resolved on a SDS-PAGE gel and analyzed with Western blot using the anti-Kbu antibody PTM-301. The chemiluminescent protein bands on the Western blot membrane are collective signals corresponding to Knbu and Kibu levels because of the promiscuity of this antibody. Nevertheless, any intensity change upon d7-isobutyrate treatment will reflect changes in the Kibu level because isobutyrate treatment induced synthesis of isobutyryl-CoA rather than n-butyryl-CoA. As shown in **Figure 4**, both whole proteome extracts and histone extracts showed increased Kibu levels on histones H3 and H4, as a result of isobutyrate treatment. Thus, Kibu is a *bona fide* histone PTM and is driven by isobutyryl-CoA. Surprisingly, under our condition, no appreciable change of

chemiluminescence intensity was observed on non-histone proteins upon isobutyrate treatment.

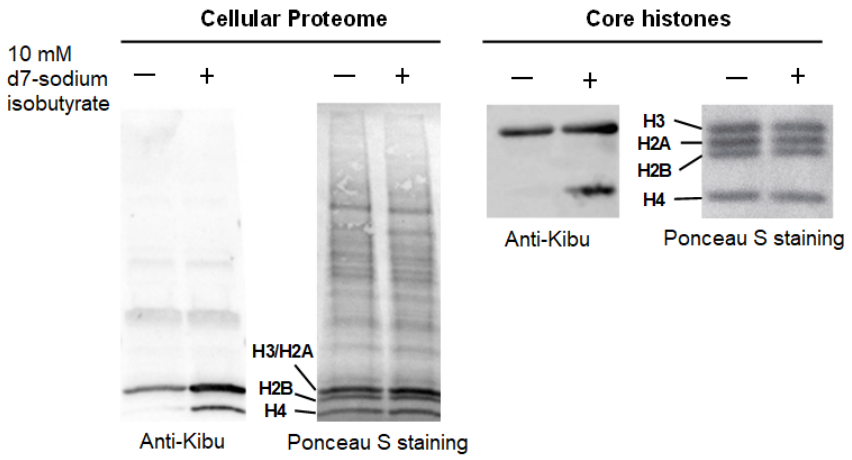

Figure 4. Detection of lysine isobutyrylation on protein lysines. HEK293T cells were treated with sodium isobutyrate to induce the synthesis of isobutyryl-CoA. Cellular proteome and core histone proteins were extracted and tested with anti-butyryllysine antibody (PTM Biolabs, Cat#PTM-301). Treatment of cells with isobutyrate induced increase of lysine isobutyrylation level on core histone proteins while no appreciable change was observed on non-histone protein isobutyrylation upon isobutyrate treatment.

To confirm histone Kibu in cells, we performed HPLC-MS/MS analysis of the histone extract (**Figure 5**). The core histones were extracted from the sodium d7-isobutyrate treated HEK293T cells and subsequently digested with trypsin. The resulting tryptic peptides were subjected to nano-HPLC/MS/MS analysis and protein sequence alignment with Mascot algorithm. Our analysis led to the identification of two modified H3 peptides, KSTGGKAPR and KQLATKAAR, which contain a mass shift of + 77.0858 Da at sites H3K14 and H3K23, respectively. This mass shift is the same as that caused by the addition

of a d7-isobutyralation, demonstrating the existence of two novel isobutyralation sites on histone H3.

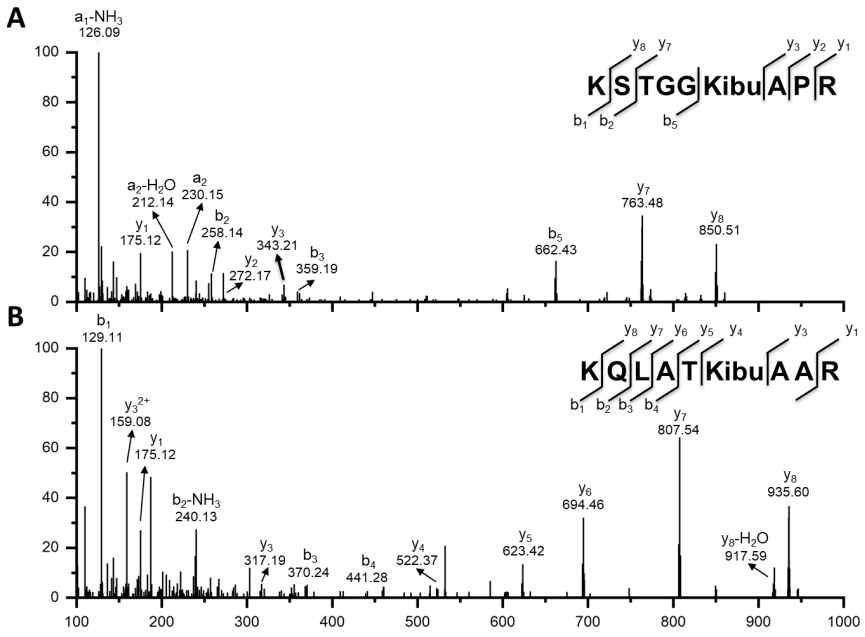

Figure 5. MS/MS spectra of histone H3Kibu14 (A) and H3Kibu23 (B) in 293T cells. The b and y ions refer to peptide backbone fragment ions containing N- and C-terminus, respectively.

The p300 acetyltransferase possesses histone isobutyrylation activity in the cell.

We moved on to test which KAT can mediate Kibu levels in cells. We focused on p300 and HAT1 as they both showed clear isobutyrylation activity on peptide substrates (**Figure 3** and **Figure 4**). To determine if they could catalyze *in cellulo* lysine isobutyrylation, we performed transient transfection of p300 and HAT1 plasmid in 293T cells and then treated the cells with sodium d7-isobutyrate. Consistent with the above observations (**Figure 4**), isobutyrate significantly increased Kibu levels in histones, suggesting isobutyrate is the source of isobutyryl group to promote isobutyrylation

(**Supplementary Figure S4, Lanes 2 and 6**). In the presence of p300 overexpression and isobutyrate treatment together, Kibu levels were further boosted (**Supplementary Figure S4, Lane 4**) especially on histone H3 region. These data suggest that histone H3 may be a major Kibu target mediated by p300. The result is consistent with previous studies that p300 acetylates multiple sites in histone H3.[124,125] Surprisingly, we did not observe any significant change in the Kibu level with HAT1 overexpression (**Supplementary Figure S4, Lane 8**). Such a difference between biochemical and *in cellulo* assay results in isobutyrylation may reflect the context dependence of HAT1 activity.

Structural insights of the HAT1 and p300 interactions with isobutyryl-CoA

To elucidate the structural basis of HATs' isobutyryltransferase activity, we generated the 1.6 Å crystal structure of the ternary complex of HAT1 with isobutyryl-CoA (IbuCoA) and histone H4(K12A) mutant peptide, referred to here as HAT1-IbuCoA-H4(K12A) (PDB ID: 6VO5) (**Table S1**). We used the H4(K12A) mutant peptide instead of the wild type counterpart to avoid any reaction intermediates between the ε-amino group of lysine12 (K12) of H4 and IbuCoA, and eventually to better resolve the electron density of the isobutyryl moiety of IbuCoA in HAT1-IbuCoA-H4(K12A). For comparison, the wild type H4K12 side chain inserts into the HAT1 active site tunnel in the crystal structure of HAT1 bound to acetyl-CoA and H4, referred to here as HAT1-AcCoA-H4 (PDB ID: 2P0W). Previous studies have shown that human HAT1 can acetylate soluble (but not nucleosomal) histone H4 at K5 and K12 positions.[126] In HAT1-IbuCoA-H4(K12A), the H4(K12A) peptide adopts a similar conformation and binding pattern with HAT1 compared to that of HAT1-AcCoA-H4 (**Figure 6A, B**), suggesting that the N-terminal sequence motif of H4 plays a crucial role in HAT1 substrate recognition and binding, and consistent with H4K12

being the preferred HAT1 acetylation site. The overall IbuCoA interaction with HAT1 is similar to that of AcCoA-HAT1 interaction observed in HAT1-AcCoA-H4, except for the adenosine ring of IbuCoA in HAT1-IbuCoA-H4(K12A), which adopts a pi-stacking interaction with Phe288 side chain of HAT1 instead of Lys284 (**Figure 6C**). The electron density omit-map for IbuCoA in the crystal structure of HAT1-IbuCoA-H4(K12A) contained clear density for the extra isobutyryl moiety of IbuCoA, thus revealing that HAT1 also accommodates IbuCoA in its active site without any structural rearrangements (**Figure 6D**).

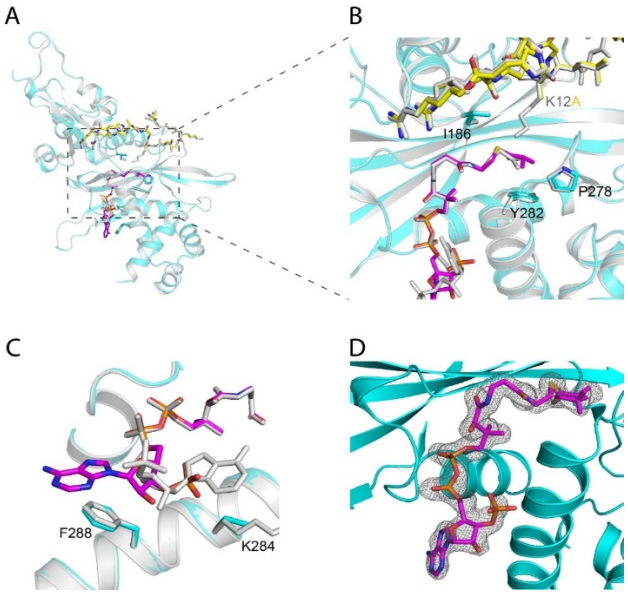

Figure 6. Crystal structure of HAT1 in complex with isobutyryl-CoA. (A) Overall fold of HAT1-IbuCoA-H4(K12A) shown in cyan, superposed on HAT1-AcCoA-H4 (PBD ID: 2P0W) shown in grey. IbuCoA and Histone H4(K12A) peptide is shown in stick representation in magenta in yellow, respectively. Acetyl-CoA and Histone H4 from HAT1-AcCoA-H4 structure (PBD ID: 2P0W) is shown in stick representation in grey. (B) Close-up view of the Isobutyryl moiety of IbuCoA binding site. (C) Close-up view of the adenosine ring of IbuCoA binding site. (D) The F_o-F_c electron density omit-map of IbuCoA

(chain B) in the crystal structure of HAT1-IbuCoA-H4(K12A), displayed as grey mesh and contoured at 2.5σ.

Similarly, p300 was previously shown to accommodate a diverse array of acyl-CoAs as substrates, and several structures of p300 in complex with acyl-CoA variants including acetyl-CoA and butyryl-CoA were reported.[105] To further corroborate the p300 isobutyryltransferase activity observed in our assays, we modeled an IbuCoA in the crystal structure of p300 bound to butyryl-CoA (PDB ID: 5LKT). Impressively, we found that IbuCoA and butyryl-CoA bound to the active pocket of p300 with the same conformation (**Supplementary Figure S5**). Clearly p300 accommodates well isobutyryl-CoA in its acyl-CoA binding pocket, accounting for the observed Kibu activity.

Isobutyrate globally affects the transcriptional profile of 293T cells

To systemically understand epigenetic changes affected by lysine isobutyrylation, we performed RNA-seq profiling on isobutyrate-treated 293T cells. Gene set enrichment analysis (GSEA) was used to compare the rank-ordered dataset of isobutyrate-treated versus control transcripts with respect to the KEGG pathways altered by isobutyrate treatment (**Figure 7 and supplementary Figure S6**). The results revealed that isobutyrate treatment caused upregulation of a number of genes associated with such important biological pathways as diabetes-related signaling, calcium signaling, hedgehog signaling, and JAK/STAT signaling. On the other hand, there were also some genes downregulated by isobutyrate which included aminoacyl-tRNA biosynthesis, mRNA splicing, DNA replication, and DNA repair.

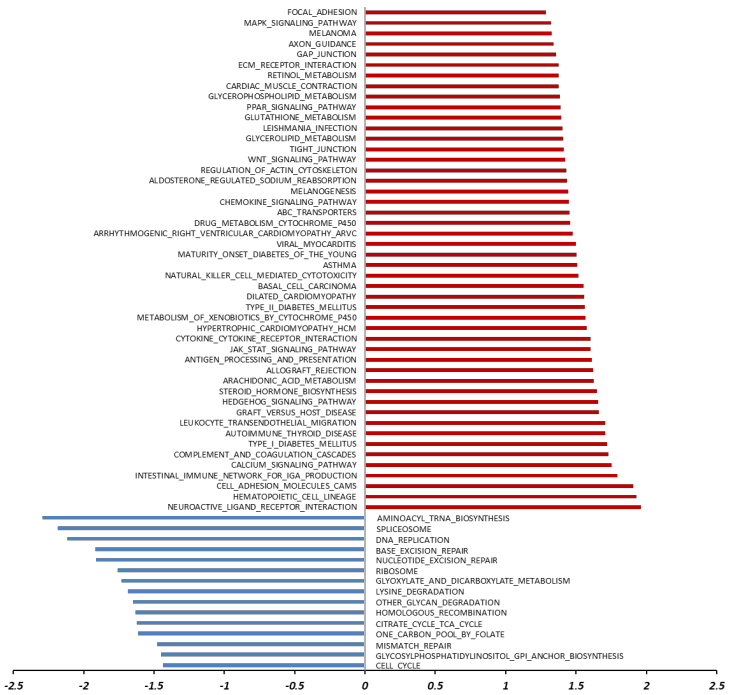

Figure 7. Enrichment analysis of the top gene sets altered by isobutyrate treatment in HEK293T cells. Significantly altered gene sets were defined with the False Discovery Rate (FDR) and p value less than 0.25 and 0.05, respectively. These genes were analyzed against the KEGG pathway for upregulation (red) and downregulation (blue).

4.4 Discussion

Histone modifications are key players in the epigenetic regulation of chromatin dynamics and transcriptional programing. Various histone PTM marks in combination create unique epigenetic patterns that are associated with transcriptional statuses of target genes.[127] Lysine butyrylation was recognized as n-butyrylation upon its discovery.[34] Later study showed that butyrylation competes with acetylation on the same lysine residue and leads to different biological outcomes.[41] Herein, we identified lysine isobutyrylation, the structural isomer of n-butyrylation, as a new PTM in histones. Although our mass

spectrometry experiment only revealed two sites in histone H3, K18 and K23, being isobutyrylated, the Western blot data suggest that histone H4 was also isobutyrylated (**Figure 5**). In future it is needed to develop isobutyryllysine-specific antibody or chemical probes and apply them to precisely map out lysine isobutyrylation sites in the chromatin histones and in the whole proteome. Both n-butyryl-CoA and isobutyryl-CoA are ample metabolites in mammalian cells but differ in their biosynthetic pathways. While n-butyryl-CoA is derived from fatty acid metabolism, isobutyryl-CoA comes from valine metabolism **(Figure 1)**. Dairy and ruminant foods are rich in branched chain fatty acids whose degradation provide another rich source of isobutyryl-CoA.[128] Although butyryl-CoA mutase enzyme has been known in prokaryotic organisms and is able to interconvert n- and iso-butyryl-CoA,[129] our blast search does not yield any possible orthologs existing in eukaryotic organisms. Indeed, treatment of 293T cells with d7-isobutyryate or valine only boosted isobutryl-CoA level, but not n-butyryl-CoA (**Supplementary Figure S1**), supporting that an isobutyryl-CoA mutase is not present in higher organisms.

The biochemical activity assays clearly showed that KAT members p300 and HAT1 catalyze lysine isobutyrylation activity *in vitro*. This is further substantiated by structural determination that both KATs bind to isobutyryl-CoA in their acetyl-CoA binding pocket. However only p300 showed cellular Kibu activity in our tested cell model. The discrepancy of HAT1 isobutyrylation activity in the biochemical assays from its lack of cellular activity may be a consequence of cellular context. HAT1 has been shown to form a protein complex with RIP1/3,[130] which may change the molecular environment of HAT1 and contribute to alterations in isobutyrylation substrate specificity in cells. It will be necessary in future to

investigate isobutyrylation activity of p300, HAT1, and other KATs (e.g. HBO1) in a broader scope and in different biological systems.

RNA-seq profiling showed that isobutyrate led to an extensive change in the expression levels of multiple genes in 293T cells. This exemplifies the intricate connection between metabolites and epigenetics: isobutyrate increases cellular levels of isobutyryl-CoA and thereby leads to isobutyrylation of nuclear histones and transcriptional changes. In terms of biophysical properties, lysine isobutyrylation may have similar effects as acetylation on chromatin structure and gene transcription: both acylations neutralize the positive charge on the lysine side chain and disrupt or weaken the electrostatic interaction between histones and DNA. As a result, the chromatin architecture becomes more loosely stacked and transcriptionally active gene sets are enhanced. At this point, it is unknown whether any reader protein modules exist to recognize isobutyryllysine and distinguish it from other lysine acylation marks. Our preliminary results showed that TAF1 bromodomain binds to acetylated H4 peptide but not isobutyrylated H4 peptide (data not shown), suggestive of possible antagonistic function of lysine isobutyrylation from acetylation. In addition, our RNA-seq data showed that certain genes are downregulated upon isobutyrate treatment. One reason for this phenomenon could be owing to the pharmacological effect of isobutyrate on cellular HDAC activities. Previous studies showed that n-butyrate, β-hydroxybutyrate and 4-phenylbutyrate all have inhibitory effects on the HDAC enzymes,[131] which would positively influence gene expression by increasing the chromatin accessibility of transcriptional factors. Likely, isobutyrate may also affect the gene expression profile through inhibiting HDACs. This study calls for a

comprehensive assessment of transcriptional and pharmacological effects of different short chain fatty acid (SCFA) molecules.

Acetate, propionate, and n-butyrate, produced by human gut microbiota directly impact on host physiology. [132] For instance, these SCFAs exhibit anti-inflammatory and anti-proliferative properties in the gastrointestinal tract, which provides novel strategies to develop anti-inflammation or anti-tumor therapeutics.[133] It will be intriguing to examine the percentage of isobutyrate molecules produced by luminal microbiota and how it affects the physiology of the intestinal epithelial cells. Protein isobutyrylation in those host cells may dynamically changes in response to the microbiota environment. During valine catabolism, degradation of isobutyryl-CoA is catalyzed by isobutyryl-CoA dehydrogenase (IBD) encoded by the *ACAD8* gene.[134] Mutations in *ACAD8* cause a rare inborn metabolic disorder, IBD deficiency, and lead to impaired isobutyryl-CoA breakdown and reduced energy production.[134] Although most IBD deficiency patients are asymptomatic, some develop severe features of dilated cardiomyopathy, hypotonia, and anemia.[135] The range of symptoms associated with IBD deficiency remain unclear, and biomarkers for IBD deficiency are being investigated to allow efficient and effective diagnosis.[136] We anticipate that isobutyryl-CoA level would increase and hence protein lysine isobutyrylation may be upregulated in patients with IBD deficiency. Further proteomic work will be warranted to screen lysine isobutyrylation and investigate its function in IBD deficiency disease models.

Supporting information for Chapter 4

Table S1. Data collection and refinement statistics.

	HAT1-IbuCoA-H4(K12A) (PDB ID: 6VO5)
Data collection[a]	
Space group	$P2_12_12$
Cell dimensions	
a, *b*, *c* (Å)	116.72, 155.63, 53.47
α, β, γ (°)	90.00, 90.00, 90.00
Resolution (Å)	48.62-1.6 (1.63-1.60)[b]
R_{merge}	0.059 (1.066)
$I/\sigma(I)$	20.3(1.9)
$CC_{1/2}$	0.999 (0.723)
Completeness (%)	99.5 (99.5)
Redundancy	8.8 (9.1)
Refinement	
Resolution (Å)	47.45-1.6
No. reflections	121983
R_{work} / R_{free}	0.170/0.197
No. atoms	6647
Protein	5452
ligand	112
peptide	189
Water	746
B factors	28.3
Protein	26.5
ligand	37.0
peptide	36.7
Water	37.5
R.m.s. deviations	
Bond lengths (Å)	0.007
Bond angles (°)	1.406

*Values in parentheses are for highest-resolution shell.

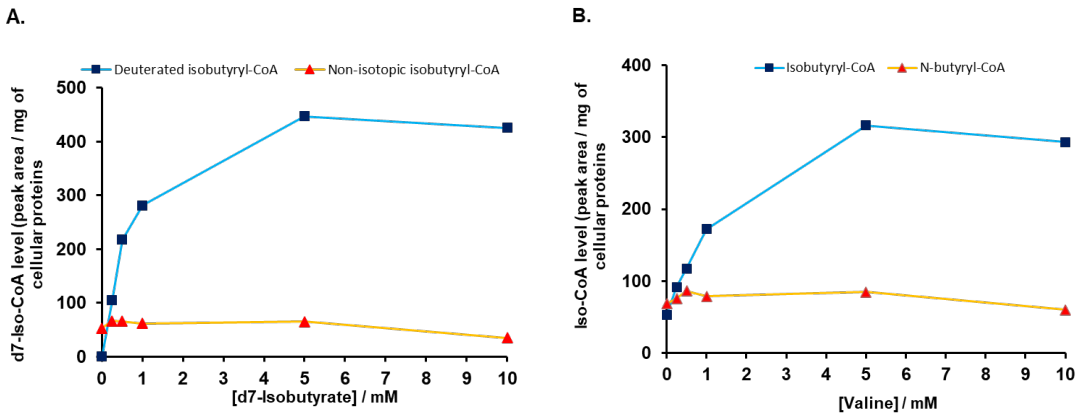

Figure S1. Cellular levels of isobutyryl-CoA correlate with isobutyrate and valine feeding. 293T cells were incubated with different concentrations of d7-isobutyrate or valine. After cell culture and lysis, isobutyryl-CoA from extracts were analyzed by HPLC-MS/MS. Of note, isobutyryl-CoA level was increased, but n-butyryl-CoA level was not affected in response to isobutyrate or valine treatment.

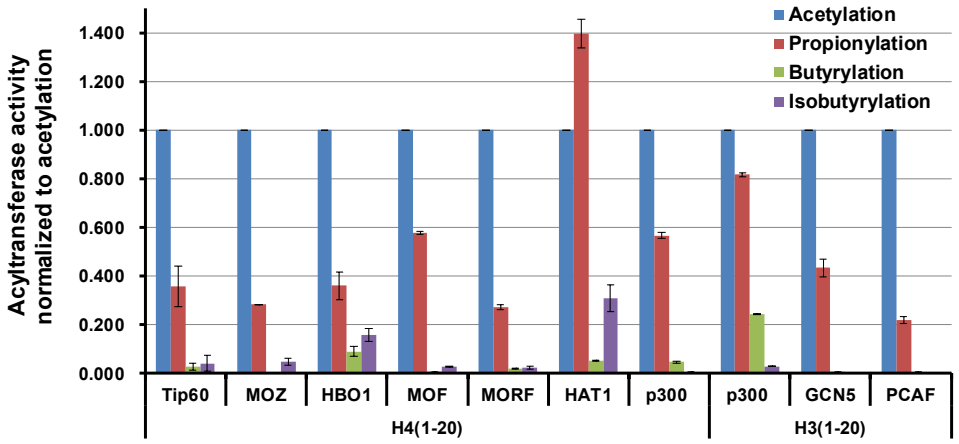

Figure S2. Relative lysine acylation activities of different KAT enzymes. Lysine acetyl-, propionyl-, nbutyryl-, and isobutyryltransferase activities of each KAT enzymes were tested using the fluorometric CPM assay, with fixed concentration of acyl-CoAs and H3(1-

20) and H4(1-20) histone peptide substrates. All tested KATs showed strong activity on lysine acetylation and appreciable activity on lysine propionylation. HAT1 showed the strongest activity of carrying out lysine isobutyrylation, about 25% of its acetyltransferase activity.

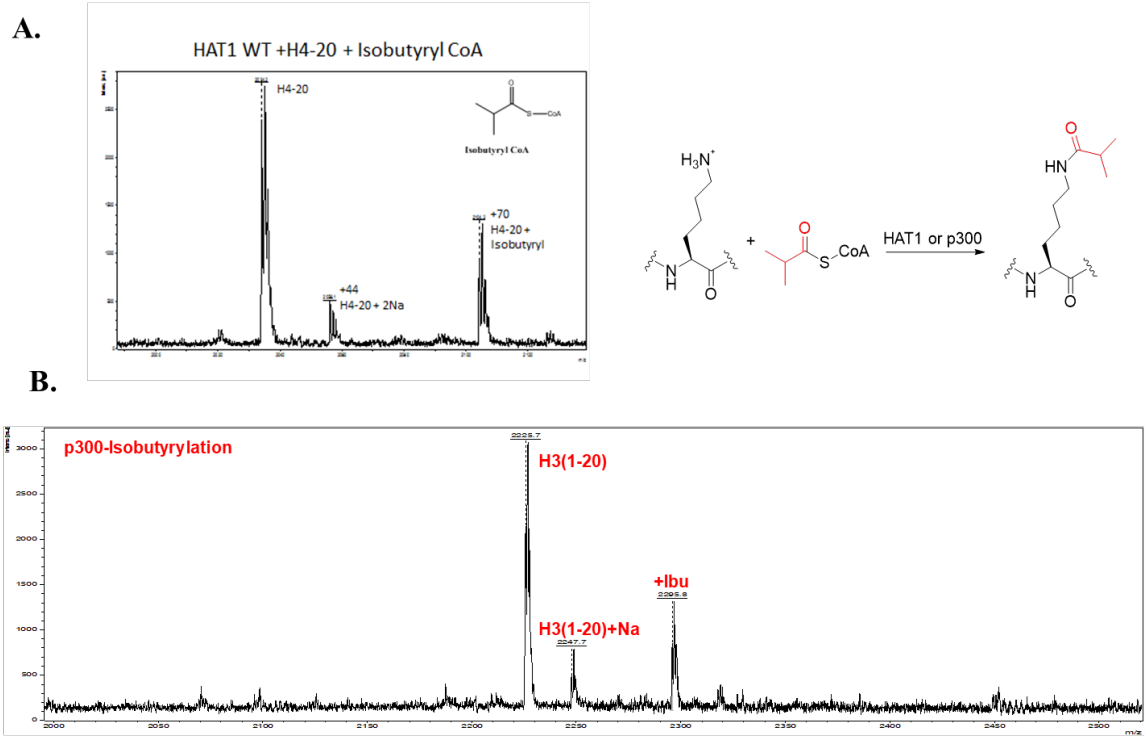

Figure S3. Isobutyrylation activity of p300 and HAT1 on the histone peptide substrates was detected by MALDI-MS. Enzymatic reaction was carried out at 30℃ for 1 h; [Enzyme]: 1 μM; H3(1-20) or H4(1-20) peptide: 50 μM; isobutyryl-CoA: 50 μM. The reaction was quenched with 10% TFA. A. MS data shows that HAT1 catalyzes histone isobutyrylation on H4 peptide. B. MS data shows that p300 catalyzes histone H3 isobutyrylation.

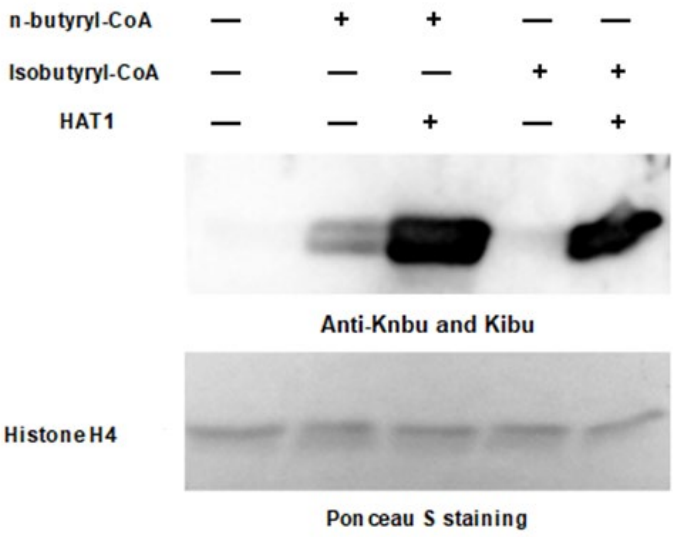

Figure S4. Western blot detection of HAT1-mediated lysine isobutyrylation using an anti nbutyryllysine antibody. Recombinant histone H4 was incubated with HAT1 and butyryl-CoA or isobutyrylCoA. Butyrylation levels on histone H4 were detected with the anti n-butyryllysine antibody from PTM BioLabs (Cat#PTM-301). The results demonstrated this antibody can detect both n- and isobutyrylation on histone lysines.

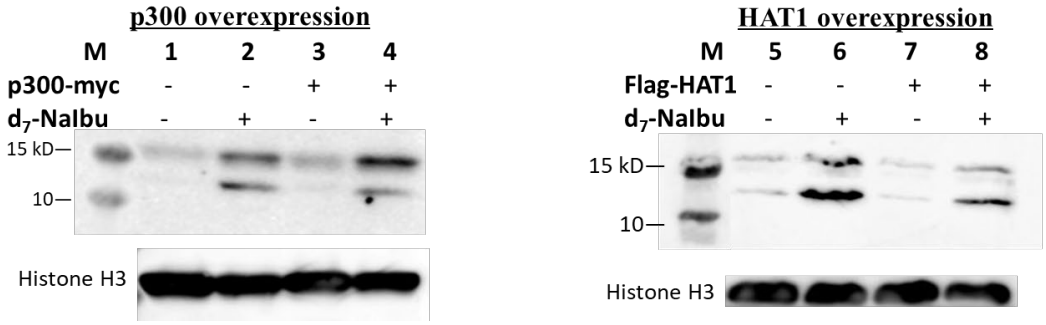

Figure S5. Effect of p300 and HAT1 overexpression on histone isobutyrylation. Histone extracts were resolved on SDS-PAGE, transferred to nitrocellulose membrane, and detected with the PTM-301 antibody.

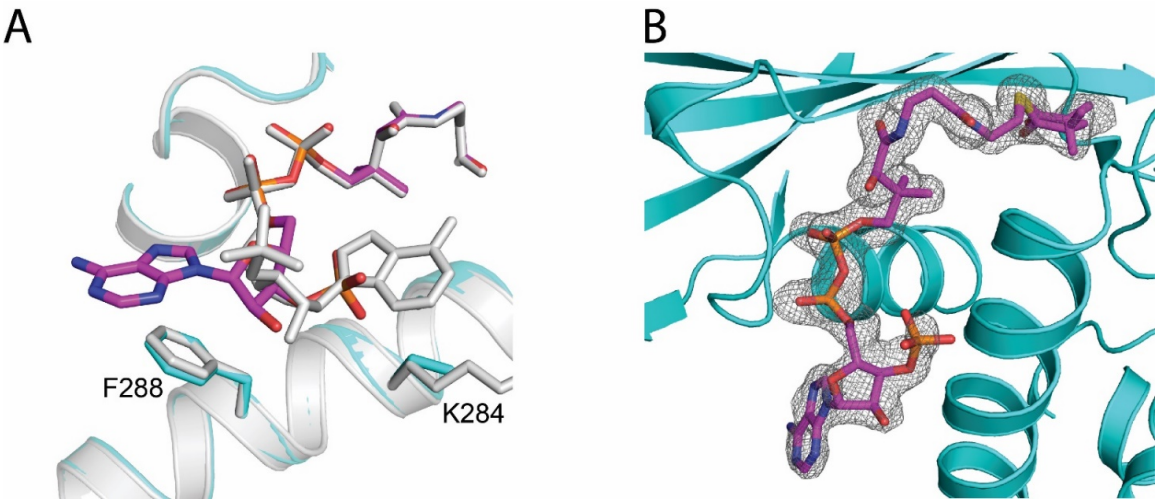

Figure S6. HAT1 interaction with IbuCoA and H4(K12A) peptide. The structure was obtained by overlaying the PDB 2P0W and PDB 6VO5. (A) Close-up view of the adenosine ring of IbuCoA binding site. (B) The Fo-Fc electron density omit-map of IbuCoA (chain B) in the crystal structure of HAT1-IbuCoAH4(K12A), displayed as grey mesh and contoured at 2.5σ.

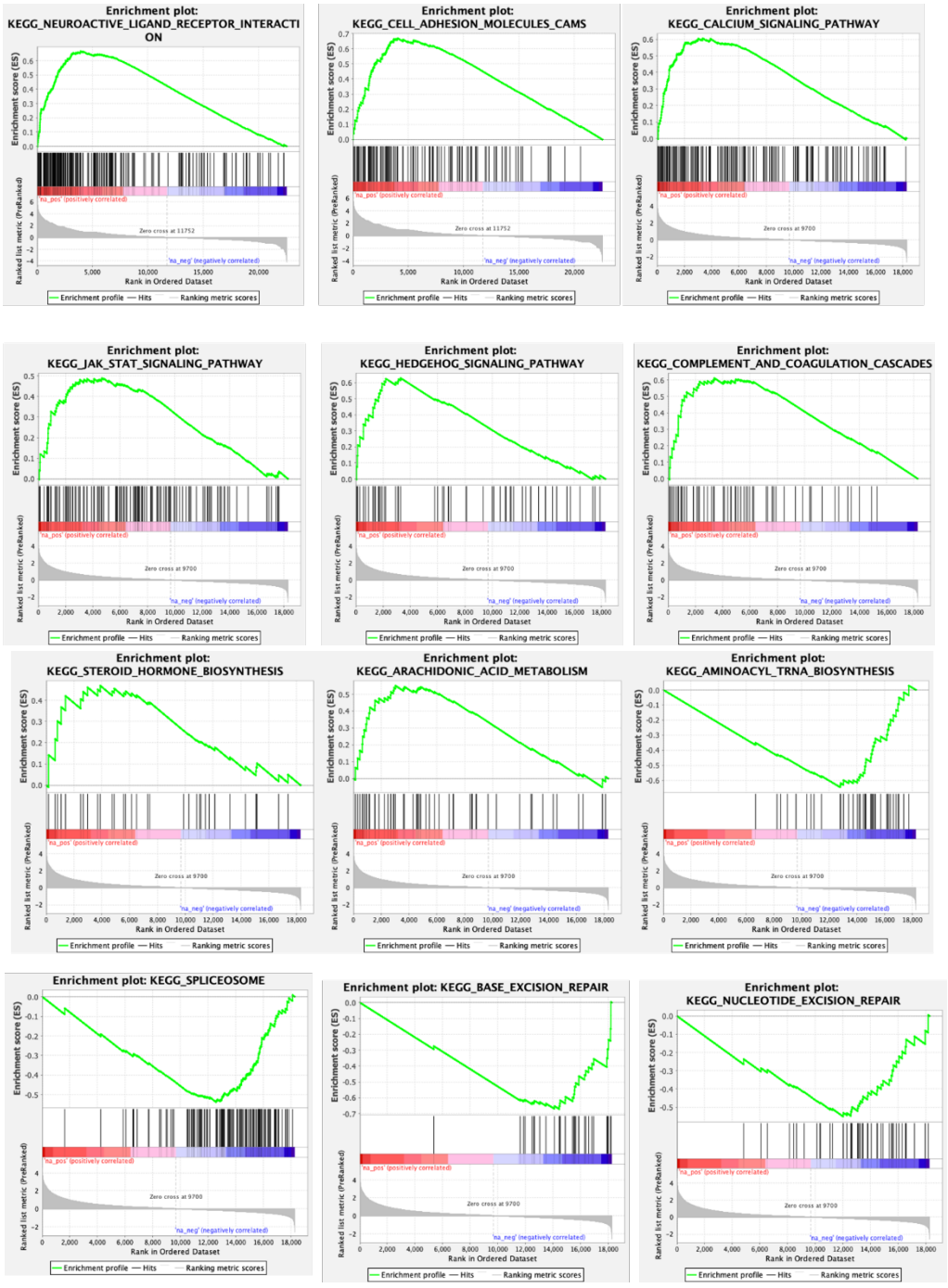

Figure S7. Gene Set Enrichment Analysis (GSEA) of signaling pathways upregulated by isobutyratetreatment of 293T cells. RNA-seq data of HEK293T cells with and without

isobutyrate treatment were submitted for GSEA. Selective pathways of our top interest are plotted.

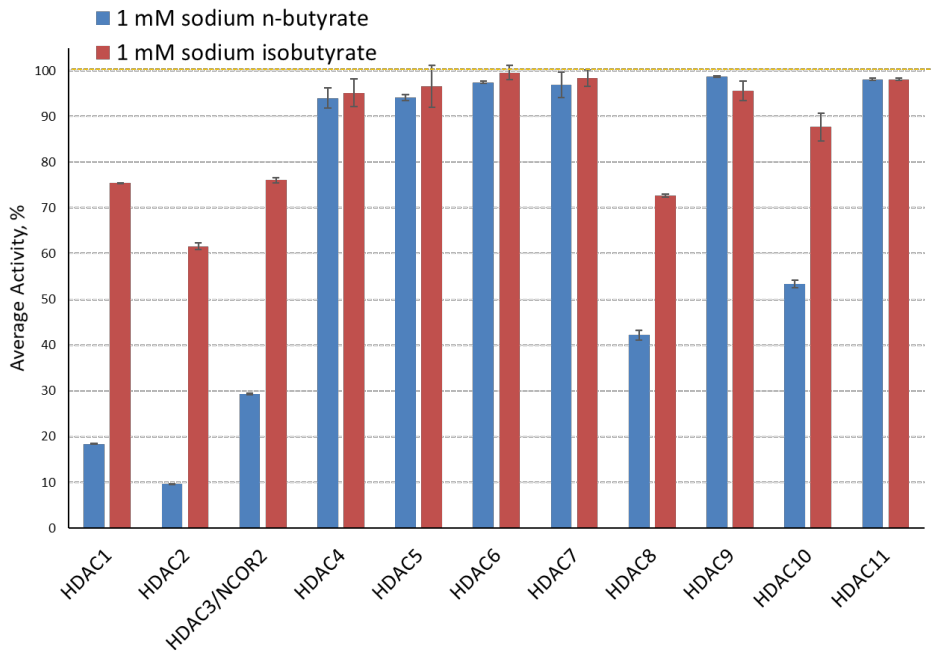

Figure S8. Effects of n-butyrate and isobutyrate on the activity of individual HDACs. Activity inhibition on HDACs 1-11 by sodium n-butyrate and sodium isobutyrate was measured at 1 mM. The experiment was done using a fluorometric assay by BPS Bioscience Inc. Results were represented by average remaining % of activity of HDACs after incubation with tested compounds. The data showed that isobutyryate was able to inhibit HDACs 1-3, 8 and 10, which are also inhibition targets of n-butyrate. However, the activities of isobutyryate were weaker than n-butyrate, with % inhibition around 20-40% of the latter's activities.

Acknowledgement

The X-ray structure determination of HAT1 was performed by Dr. Levon Halabelian, Dr. Hong Zeng and Dr. Cheryl H. Arrowsmith at the Structural Genomics

Consortium, University of Toronto. Analysis of butyryl-CoA and isobutyryl-CoA in the cell was done by Dr. Zhen Han, and Dr. Xiangkun Yang in Dr. Michael Bartlett's laboratory. The MS/MS identification of histone isobutyrylation sites was done by Dr. Jun Ding and Dr. Yingming Zhao at University of Chicago. Isobutyryl-CoA was synthesized by Dr. Maomao He. The RNA-seq data were acquired and analyzed by Dr. Nawei Zhang and Dr. Minkui Luo at Memorial Sloan Kettering Cancer Center. Dr. Zhen Han and Dr. Liza Ngo performed the early stage experimental studies of the work.

CHAPTER 5

SUMMARY AND FUTURE DIRECTIONS

HATs are important regulators of histone PTMs and have gained increasing attention for their cellular function and physiological roles in various diseases. Deregulation especially overexpression of HATs has been seen many types of cancer, and therefore, pharmaceutical industry and academic research have actively pursued to understand how HATs contribute to cancer progression develop strategies to inhibit these enzymes. In addition, HATs are found to catalyze different acylations other than the canonical acetylation (e.g., propionylation, crotonylation, succinylation), which expands study scope of HATs and gain more insight into gene regulation. Despite great progress that has been made in recent years, the "histone code" or histone marks and their functional consequences are still unknown. Plus, the complexity of cellular environment may pose challenges to the study, for the catalytic behavior and substrate specificity of HATs could alter in histone octomer, and the nucleosome. Other chromatin modifiers, such as PRMTs, can coordinate with HATs and deposit or remove different histone PTMs. In this context, it is not completely studied how HATs are regulated and what can influence their cellular functions.

In this work, we sought to understand how HATs are influenced by different CoA-based compounds. We profiled structure-activity relationships between acyl-CoAs and HATs *in vitro*, and found correlation between acyl-chain length of linear acyl-CoAs and their potency in inhibiting HATs. While short- and median-chain acyl-CoAs have shown

selectivity towards HATs, long-chain acyl-CoAs are poorly selective pan-acetylation inhibitors. We also observed that unsaturation could facilitate inhibition and selectivity of acyl-CoA to p300, possibly due to the cationic binding pocket or aromatic environment surrounding the acyl chain. This provides a novel strategy to design and develop CoA-based compounds as selective and potent p300 inhibitors. CoA derivatives have long been considered cell-impermeable owing to negatively charged phosphate groups on CoA moiety. However, it is feasible to neutralize negative charges by appending cationic groups or aromatic groups on S-warhead to promote drug delivery in cells and result in inhibition of histone acetylation, as exemplified by Spd-CoA.[83] Whether or not this strategy could work for more cell lines and improve potency has not been completed studied yet.

Apart from developing novel CoA derivatives as HAT inhibitors, we discovered a new histone PTM, histone lysine isobutyrylation, and its modification sites which differ from its isomeric modification, histone n-butyrylation. This modification involves isobutyryl-CoA as the cofactor which is produced during valine and isobutyrate metabolism. Despite lack of specific antibody to detect histone isobutyrylation in cells, we were able to adopt HPLC-MS/MS strategy to identify substrates and to discover HATs that are responsible for this new modification. We were unable to obtain its cellular abundance compared with lysine acetylation, and it is not clear why HAT1 could catalyze histone isobutrylation in biochemical assays but failed in cells. These are the questions that may need to address so that we can obtain in-depth knowledge of histone PTM.

In summary, we have examined inhibition of different natural acyl-CoAs and synthetic CoA derivatives to HATs. We have also expanded outlook of histone PTM by

identifying a new histone acylation, lysine isobutyrylation. The following addresses some of these findings and suggests future directions:

(1) Structural optimizations and further development of CoA-based HAT inhibitors

We investigated structure-activity relationship (SAR) between acyl-CoAs and HAT representatives, and observed correlation between length of linear chain and potency of linear saturated acyl-CoAs. Unsaturation and branched structure could also affect potency, varying from different HAT families. Given the limited number of tested enzymes, one can expand the screening scope of HATs to further verify specificity of CoA derivatives, and determine the mode of inhibition of the hit compounds since HATs utilize different substrates and catalytic mechanisms. On the basis of more comprehensive studies, one can draw detailed conclusions on SAR of CoA-based probes and HATs which can be exploit to perform structural optimizations.

While it remains unknown whether A433-CoA is cell permeable, one can identify cellular metabolites pertaining to CoA-based structure. Enhancing cell permeability can also be accomplished by appending nonpeptide S-substituents, as evidenced by a cell-permeable CoA-based HAT inhibitor Spd-CoA[83] in which the amine group counteracts negative charges on CoA moiety. Therefore, one may append positive charges on acyl chain such as varied polyamine structures and perform cell permeability study or cellular metabolism study. Also, it would be valuable to examine crystal structures of A433-CoA or other candidates with HATs to gain insight into molecular basis of ligand-receptor binding. Binding affinity could also be quantified to analyze cooperativity of drug-target interactions.

Our results of cellular data regarding A433-CoA reflects inhibition of histone acetylation in PC-3 cell line that overexpresses p300/CBP. One should also check its inhibition of acetylation in other cell lines, including noncancerous and cancerous ones. Since histone acetylation regulates gene transcription, it would be of great interest to investigate the effects of drug(s) on transcriptome and transcription of specific genes at the mRNA level.

(2) Development of chemical probes for profiling lysine isobutyrylation in cells

We have found a novel histone mark lysine isobutyrylation which expands the scope of histone acylations and paves way for study of butyrate and isobutyrate metabolism. The research was conducted with canonical HPLC-MS/MS and immunoblot approaches. However, we met some challenges in detecting cellular lysine isobutyrylation with specific antibodies that was not available during the time of study. We did find an alternative, anti-n-butyrylated lysine antibody, but it resulted in cross-reactivity with lysine n-butyrylation and therefore poor quality of the antibody. In addition to antibody-based studies, a great deal of progress has been made in bioorthogonal labeling in discovery of novel modifications on proteins. One would utilize protein engineering and metabolic labeling under physiological conditions to develop isobutyryl-CoA-based probes to profile lysine isobutyrylation. The chemical biology approach would supplement antibody-based studies, and may be more specific in recognizing protein modifications.

REFERENCES

1 Liu, B., Yip, R. K. & Zhou, Z. Chromatin remodeling, DNA damage repair and aging. *Curr Genomics* **13**, 533-547, doi:10.2174/138920212803251373 (2012).

2 van Steensel, B. Chromatin: constructing the big picture. *EMBO J* **30**, 1885-1895, doi:10.1038/emboj.2011.135 (2011).

3 Hizume, K., Yoshimura, S. H. & Takeyasu, K. Linker Histone H1 per se Can Induce Three-Dimensional Folding of Chromatin Fiber. *Biochemistry* **44**, 12978-12989, doi:10.1021/bi050623v (2005).

4 Heermann, D. W. Mitotic chromosome structure. *Experimental cell research* **318**, 1381-1385, doi:10.1016/j.yexcr.2012.03.027 (2012).

5 Weinhold, B. Epigenetics: the science of change. *Environ Health Perspect* **114**, A160-A167, doi:10.1289/ehp.114-a160 (2006).

6 Herrmann, F., Pably, P., Eckerich, C., Bedford, M. T. & Fackelmayer, F. O. Human protein arginine methyltransferases in vivo – distinct properties of eight canonical members of the PRMT family. *Journal of Cell Science* **122**, 667, doi:10.1242/jcs.039933 (2009).

7 Ezhkova, E. *et al.* EZH1 and EZH2 cogovern histone H3K27 trimethylation and are essential for hair follicle homeostasis and wound repair. *Genes & development* **25**, 485-498, doi:10.1101/gad.2019811 (2011).

8 Marmorstein, R. & Trievel, R. C. Histone modifying enzymes: structures, mechanisms, and specificities. *Biochim Biophys Acta* **1789**, 58-68, doi:10.1016/j.bbagrm.2008.07.009 (2009).

9 Wang, P., Wang, Z. & Liu, J. Role of HDACs in normal and malignant hematopoiesis. *Molecular Cancer* **19**, 5, doi:10.1186/s12943-019-1127-7 (2020).

10 Rossetto, D., Avvakumov, N. & Côté, J. Histone phosphorylation: a chromatin modification involved in diverse nuclear events. *Epigenetics* **7**, 1098-1108, doi:10.4161/epi.21975 (2012).

11 Naqvi, S. *et al.* Characterization of the cellular action of the MSK inhibitor SB-747651A. *Biochem J* **441**, 347-357, doi:10.1042/bj20110970 (2012).

12 Meas, R. & Mao, P. Histone ubiquitylation and its roles in transcription and DNA damage response. *DNA Repair (Amst)* **36**, 36-42, doi:10.1016/j.dnarep.2015.09.016 (2015).

13 Yau, T.-Y., Molina, O. & Courey, A. J. SUMOylation in development and neurodegeneration. *Development* **147**, dev175703, doi:10.1242/dev.175703 (2020).

14 Furdas, S. D., Kannan, S., Sippl, W. & Jung, M. Small molecule inhibitors of histone acetyltransferases as epigenetic tools and drug candidates. *Arch Pharm (Weinheim)* **345**, 7-21, doi:10.1002/ardp.201100209 (2012).

15 Narita, T., Weinert, B. T. & Choudhary, C. Functions and mechanisms of non-histone protein acetylation. *Nat Rev Mol Cell Biol* **20**, 156-174, doi:10.1038/s41580-018-0081-3 (2019).

16 Hull, E. E., Montgomery, M. R. & Leyva, K. J. HDAC Inhibitors as Epigenetic Regulators of the Immune System: Impacts on Cancer Therapy and Inflammatory Diseases. *Biomed Res Int* **2016**, 8797206, doi:10.1155/2016/8797206 (2016).

17 Seto, E. & Yoshida, M. Erasers of histone acetylation: the histone deacetylase enzymes. *Cold Spring Harbor perspectives in biology* **6**, a018713-a018713, doi:10.1101/cshperspect.a018713 (2014).

18 Oike, T. *et al.* C646, a selective small molecule inhibitor of histone acetyltransferase p300, radiosensitizes lung cancer cells by enhancing mitotic catastrophe. *Radiother Oncol* **111**, 222-227, doi:10.1016/j.radonc.2014.03.015 (2014).

19 Lasko, L. M. *et al.* Discovery of a selective catalytic p300/CBP inhibitor that targets lineage-specific tumours. *Nature* **550**, 128-132, doi:10.1038/nature24028 (2017).

20 Yang, Y. *et al.* Discovery of Highly Potent, Selective, and Orally Efficacious p300/CBP Histone Acetyltransferases Inhibitors. *J Med Chem* **63**, 1337-1360, doi:10.1021/acs.jmedchem.9b01721 (2020).

21 Liu, X. *et al.* The structural basis of protein acetylation by the p300/CBP transcriptional coactivator. *Nature* **451**, 846-850, doi:10.1038/nature06546 (2008).

22 Lau, O. D. *et al.* HATs off: selective synthetic inhibitors of the histone acetyltransferases p300 and PCAF. *Mol Cell* **5**, 589-595 (2000).

23 Mai, A. *et al.* Small-molecule inhibitors of histone acetyltransferase activity: identification and biological properties. *J Med Chem* **49**, 6897-6907, doi:10.1021/jm060601m (2006).

24 Voss, A. K. & Thomas, T. Histone Lysine and Genomic Targets of Histone Acetyltransferases in Mammals. *BioEssays : news and reviews in molecular, cellular and developmental biology* **40**, e1800078, doi:10.1002/bies.201800078 (2018).

25 Haigney, A., Ricketts, M. D. & Marmorstein, R. Dissecting the Molecular Roles of Histone Chaperones in Histone Acetylation by Type B Histone Acetyltransferases (HAT-B). *J Biol Chem* **290**, 30648-30657, doi:10.1074/jbc.M115.688523 (2015).

26 Sapountzi, V. & Côté, J. MYST-family histone acetyltransferases: beyond chromatin. *Cell Mol Life Sci* **68**, 1147-1156, doi:10.1007/s00018-010-0599-9 (2011).

27 Salah Ud-Din, A. I., Tikhomirova, A. & Roujeinikova, A. Structure and Functional Diversity of GCN5-Related N-Acetyltransferases (GNAT). *Int J Mol Sci* **17**, doi:10.3390/ijms17071018 (2016).

28 Dutta, R., Tiu, B. & Sakamoto, K. M. CBP/p300 acetyltransferase activity in hematologic malignancies. *Mol Genet Metab* **119**, 37-43, doi:10.1016/j.ymgme.2016.06.013 (2016).

29 Ott, M. & Verdin, E. HAT trick: p300, small molecule, inhibitor. *Chem Biol* **17**, 417-418, doi:10.1016/j.chembiol.2010.05.002 (2010).

30 Wang, F., Marshall, C. B. & Ikura, M. Transcriptional/epigenetic regulator CBP/p300 in tumorigenesis: structural and functional versatility in target recognition. *Cell Mol Life Sci* **70**, 3989-4008, doi:10.1007/s00018-012-1254-4 (2013).

31 Parthun, M. R. Hat1: the emerging cellular roles of a type B histone acetyltransferase. *Oncogene* **26**, 5319-5328, doi:10.1038/sj.onc.1210602 (2007).

32 Jin, X., Tian, S. & Li, P. Histone Acetyltransferase 1 Promotes Cell Proliferation and Induces Cisplatin Resistance in Hepatocellular Carcinoma. *Oncology Research Featuring Preclinical and Clinical Cancer Therapeutics* **25**, 939-946, doi:10.3727/096504016X14809827856524 (2017).

33 Fan, P. *et al.* Overexpressed histone acetyltransferase 1 regulates cancer immunity by increasing programmed death-ligand 1 expression in pancreatic cancer. *Journal of Experimental & Clinical Cancer Research* **38**, 47, doi:10.1186/s13046-019-1044-z (2019).

34 Chen, Y. *et al.* Lysine propionylation and butyrylation are novel post-translational modifications in histones. *Mol Cell Proteomics* **6**, 812-819, doi:10.1074/mcp.M700021-MCP200 (2007).

35 Dai, L. *et al.* Lysine 2-hydroxyisobutyrylation is a widely distributed active histone mark. *Nature Chemical Biology* **10**, 365-370, doi:10.1038/nchembio.1497 (2014).

36 Xie, Z. *et al.* Lysine succinylation and lysine malonylation in histones. *Mol Cell Proteomics* **11**, 100-107, doi:10.1074/mcp.M111.015875 (2012).

37 Tan, M. *et al.* Lysine glutarylation is a protein posttranslational modification regulated by SIRT5. *Cell metabolism* **19**, 605-617, doi:10.1016/j.cmet.2014.03.014 (2014).

38 Wan, J., Liu, H., Chu, J. & Zhang, H. Functions and mechanisms of lysine crotonylation. *Journal of cellular and molecular medicine* **23**, 7163-7169, doi:10.1111/jcmm.14650 (2019).

39 Xie, Z. *et al.* Metabolic Regulation of Gene Expression by Histone Lysine β-Hydroxybutyrylation. *Molecular cell* **62**, 194-206, doi:10.1016/j.molcel.2016.03.036 (2016).

40 Sabari, B. R., Zhang, D., Allis, C. D. & Zhao, Y. Metabolic regulation of gene expression through histone acylations. *Nat Rev Mol Cell Biol* **18**, 90-101, doi:10.1038/nrm.2016.140 (2017).

41 Goudarzi, A. *et al.* Dynamic Competing Histone H4 K5K8 Acetylation and Butyrylation Are Hallmarks of Highly Active Gene Promoters. *Mol. Cell* **62**, 169-180, doi:10.1016/j.molcel.2016.03.014 (2016).

42 Hodson, L. & Gunn, P. J. The regulation of hepatic fatty acid synthesis and partitioning: the effect of nutritional state. *Nature Reviews Endocrinology* **15**, 689-700, doi:10.1038/s41574-019-0256-9 (2019).

43 Załęski, A., Banaszkiewicz, A. & Walkowiak, J. Butyric acid in irritable bowel syndrome. *Prz Gastroenterol* **8**, 350-353, doi:10.5114/pg.2013.39917 (2013).

44 Zimmerman, M. A. *et al.* Butyrate suppresses colonic inflammation through HDAC1-dependent Fas upregulation and Fas-mediated apoptosis of T cells. *American Journal of Physiology-Gastrointestinal and Liver Physiology* **302**, G1405-G1415, doi:10.1152/ajpgi.00543.2011 (2012).

45 He, B. & Moreau, R. Lipid-regulating properties of butyric acid and 4-phenylbutyric acid: Molecular mechanisms and therapeutic applications. *Pharmacological Research* **144**, 116-131, doi:https://doi.org/10.1016/j.phrs.2019.04.002 (2019).

46 Verdone, L., Agricola, E., Caserta, M. & Di Mauro, E. Histone acetylation in gene regulation. *Briefings in Functional Genomics* **5**, 209-221, doi:10.1093/bfgp/ell028 (2006).

47 Carrozza, M. J., Utley, R. T., Workman, J. L. & Cote, J. The diverse functions of histone acetyltransferase complexes. *Trends Genet* **19**, 321-329, doi:10.1016/S0168-9525(03)00115-X (2003).

48 Wapenaar, H. & Dekker, F. J. Histone acetyltransferases: challenges in targeting bi-substrate enzymes. *Clin Epigenetics* **8**, 59, doi:10.1186/s13148-016-0225-2 (2016).

49 Kimura, A., Matsubara, K. & Horikoshi, M. A Decade of Histone Acetylation: Marking Eukaryotic Chromosomes with Specific Codes. *The Journal of Biochemistry* **138**, 647-662, doi:10.1093/jb/mvi184 (2005).

50 Segal, I. *et al.* A straightforward approach for bioorthogonal labeling of proteins and organelles in live mammalian cells, using a short peptide tag. *BMC Biology* **18**, 5, doi:10.1186/s12915-019-0708-7 (2020).

51 Di Cerbo, V. & Schneider, R. Cancers with wrong HATs: the impact of acetylation. *Briefings in Functional Genomics* **12**, 231-243, doi:10.1093/bfgp/els065 (2013).

52 Montgomery, D. C., Sorum, A. W., Guasch, L., Nicklaus, M. C. & Meier, J. L. Metabolic Regulation of Histone Acetyltransferases by Endogenous Acyl-CoA Cofactors. *Chem Biol* **22**, 1030-1039, doi:10.1016/j.chembiol.2015.06.015 (2015).

53 Van den Bulcke, T. *et al.* Data mining methods for classification of Medium-Chain Acyl-CoA dehydrogenase deficiency (MCADD) using non-derivatized tandem MS

neonatal screening data. *Journal of Biomedical Informatics* **44**, 319-325, doi:https://doi.org/10.1016/j.jbi.2010.12.001 (2011).

54 Zhang, Z. *et al.* Identification of lysine succinylation as a new post-translational modification. *Nat Chem Biol* **7**, 58-63, doi:10.1038/nchembio.495 (2011).

55 Thompson, P. R. *et al.* Regulation of the p300 HAT domain via a novel activation loop. *Nat. Struct. Mol. Biol.* **11**, 308-315 (2004).

56 Ngo, L., Wu, J., Yang, C. & Zheng, Y. G. Effective Quenchers Are Required to Eliminate the Interference of Substrate: Cofactor Binding in the HAT Scintillation Proximity Assay. *Assay Drug Dev Technol* **13**, 210-220, doi:10.1089/adt.2015.636 (2015).

57 Rath, S. *et al.* Inhibition of histone/lysine acetyltransferase activity kills CoCl2-treated and hypoxia-exposed gastric cancer cells and reduces their invasiveness. *Int J Biochem Cell Biol* **82**, 28-40, doi:10.1016/j.biocel.2016.11.014 (2017).

58 Montgomery, D. C., Sorum, A. W. & Meier, J. L. Chemoproteomic Profiling of Lysine Acetyltransferases Highlights an Expanded Landscape of Catalytic Acetylation. *Journal of the American Chemical Society* **136**, 8669-8676, doi:10.1021/ja502372j (2014).

59 Simithy, J. *et al.* Characterization of histone acylations links chromatin modifications with metabolism. *Nature Communications* **8**, 1141, doi:10.1038/s41467-017-01384-9 (2017).

60 Wang, Y. *et al.* KAT2A coupled with the α-KGDH complex acts as a histone H3 succinyltransferase. *Nature* **552**, 273-277, doi:10.1038/nature25003 (2017).

61 Liu, X. *et al.* MOF as an evolutionarily conserved histone crotonyltransferase and transcriptional activation by histone acetyltransferase-deficient and crotonyltransferase-competent CBP/p300. *Cell Discovery* **3**, 17016, doi:10.1038/celldisc.2017.16 (2017).

62 Sabari, B. R. *et al.* Intracellular crotonyl-CoA stimulates transcription through p300-catalyzed histone crotonylation. *Mol Cell* **58**, 203-215, doi:10.1016/j.molcel.2015.02.029 (2015).

63 Kaczmarska, Z. *et al.* Structure of p300 in complex with acyl-CoA variants. *Nature chemical biology* **13**, 21-29, doi:10.1038/nchembio.2217 (2017).

64 Smith, R. H. & Powell, G. L. The critical micelle concentration of some physiologically important fatty acyl-coenzyme A's as a function of chain length. *Archives of biochemistry and biophysics* **244**, 357-360, doi:10.1016/0003-9861(86)90124-4 (1986).

65 Jenuwein, T. & Allis, C. D. Translating the histone code. *Science* **293**, 1074-1080, doi:10.1126/science.1063127 (2001).

66 Kumar, R., Li, D. Q., Muller, S. & Knapp, S. Epigenomic regulation of oncogenesis by chromatin remodeling. *Oncogene* **35**, 4423-4436, doi:10.1038/onc.2015.513 (2016).

67 Bannister, A. J. & Kouzarides, T. Regulation of chromatin by histone modifications. *Cell Res* **21**, 381-395, doi:10.1038/cr.2011.22 (2011).

68 Zentner, G. E. & Henikoff, S. Regulation of nucleosome dynamics by histone modifications. *Nat Struct Mol Biol* **20**, 259-266, doi:10.1038/nsmb.2470 (2013).

69 Jih, G. *et al.* Unique roles for histone H3K9me states in RNAi and heritable silencing of transcription. *Nature*, doi:10.1038/nature23267 (2017).

70 Tikhanovich, I. *et al.* Arginine methylation regulates c-Myc-dependent transcription by altering promoter recruitment of the acetyltransferase p300. *J Biol Chem*, doi:10.1074/jbc.M117.797928 (2017).

71 Natale, F. *et al.* Identification of the elementary structural units of the DNA damage response. *Nat Commun* **8**, 15760, doi:10.1038/ncomms15760 (2017).

72 Li, L. & Wang, Y. Cross-talk between the H3K36me3 and H4K16ac histone epigenetic marks in DNA double-strand break repair. *J Biol Chem* **292**, 11951-11959, doi:10.1074/jbc.M117.788224 (2017).

73 Yang, Q. *et al.* G9a coordinates with the RPA complex to promote DNA damage repair and cell survival. *Proc Natl Acad Sci U S A*, doi:10.1073/pnas.1700694114 (2017).

74 Zhang, J., Shen, L. & Sun, L. Q. The regulation of radiosensitivity by p53 and its acetylation. *Cancer Lett* **363**, 108-118, doi:10.1016/j.canlet.2015.04.015 (2015).

75 Faiola, F. *et al.* Dual regulation of c-Myc by p300 via acetylation-dependent control of Myc protein turnover and coactivation of Myc-induced transcription. *Mol Cell Biol* **25**, 10220-10234, doi:10.1128/MCB.25.23.10220-10234.2005 (2005).

76 Pejanovic, N. *et al.* Regulation of nuclear factor kappaB (NF-kappaB) transcriptional activity via p65 acetylation by the chaperonin containing TCP1 (CCT). *PLoS One* **7**, e42020, doi:10.1371/journal.pone.0042020 (2012).

77 Sun, X. J., Man, N., Tan, Y., Nimer, S. D. & Wang, L. The Role of Histone Acetyltransferases in Normal and Malignant Hematopoiesis. *Front Oncol* **5**, 108, doi:10.3389/fonc.2015.00108 (2015).

78 Toth, M., Boros, I. M. & Balint, E. Elevated level of lysine 9-acetylated histone H3 at the MDR1 promoter in multidrug-resistant cells. *Cancer Sci* **103**, 659-669, doi:10.1111/j.1349-7006.2012.02215.x (2012).

79 Balasubramanyam, K., Swaminathan, V., Ranganathan, A. & Kundu, T. K. Small molecule modulators of histone acetyltransferase p300. *J Biol Chem* **278**, 19134-19140, doi:10.1074/jbc.M301580200 (2003).

80 Balasubramanyam, K. *et al.* Curcumin, a novel p300/CREB-binding protein-specific inhibitor of acetyltransferase, represses the acetylation of histone/nonhistone proteins and histone acetyltransferase-dependent chromatin transcription. *J Biol Chem* **279**, 51163-51171, doi:10.1074/jbc.M409024200 (2004).

81 Balasubramanyam, K. *et al.* Polyisoprenylated benzophenone, garcinol, a natural histone acetyltransferase inhibitor, represses chromatin transcription and alters global gene expression. *J Biol Chem* **279**, 33716-33726, doi:10.1074/jbc.M402839200 (2004).

82 Tanner, K. G., Langer, M. R., Kim, Y. & Denu, J. M. Kinetic mechanism of the histone acetyltransferase GCN5 from yeast. *J Biol Chem* **275**, 22048-22055, doi:10.1074/jbc.M002893200 (2000).

83 Bandyopadhyay, K. *et al.* Spermidinyl-CoA-based HAT inhibitors block DNA repair and provide cancer-specific chemo- and radiosensitization. *Cell cycle (Georgetown, Tex.)* **8**, 2779-2788, doi:10.4161/cc.8.17.9416 (2009).

84 Bowers, E. M. *et al.* Virtual ligand screening of the p300/CBP histone acetyltransferase: identification of a selective small molecule inhibitor. *Chem Biol* **17**, 471-482, doi:10.1016/j.chembiol.2010.03.006 (2010).

85 Sagar, V., Zheng, W., Thompson, P. R. & Cole, P. A. Bisubstrate analogue structure–activity relationships for p300 histone acetyltransferase inhibitors. *Bioorganic & Medicinal Chemistry* **12**, 3383-3390, doi:https://doi.org/10.1016/j.bmc.2004.03.070 (2004).

86 Kwie, F. H. *et al.* New potent bisubstrate inhibitors of histone acetyltransferase p300: design, synthesis and biological evaluation. *Chem Biol Drug Des* **77**, 86-92, doi:10.1111/j.1747-0285.2010.01056.x (2011).

87 Zheng, Y. *et al.* Synthesis and evaluation of a potent and selective cell-permeable p300 histone acetyltransferase inhibitor. *J Am Chem Soc* **127**, 17182-17183, doi:10.1021/ja0558544 (2005).

88 Guidez, F. *et al.* Histone acetyltransferase activity of p300 is required for transcriptional repression by the promyelocytic leukemia zinc finger protein. *Mol Cell Biol* **25**, 5552-5566, doi:10.1128/MCB.25.13.5552-5566.2005 (2005).

89 Liu, X. *et al.* The structural basis of protein acetylation by the p300/CBP transcriptional coactivator. *Nature* **451**, 846, doi:10.1038/nature06546 https://www.nature.com/articles/nature06546#supplementary-information (2008).

90 Casero, R. A., Jr. & Woster, P. M. Recent advances in the development of polyamine analogues as antitumor agents. *Journal of medicinal chemistry* **52**, 4551-4573, doi:10.1021/jm900187v (2009).

91 Aebersold, R. *et al.* How many human proteoforms are there? *Nat. Chem. Biol.* **14**, 206-214, doi:10.1038/Nchembio.2576 (2018).

92 Verdin, E. & Ott, M. 50 years of protein acetylation: from gene regulation to epigenetics, metabolism and beyond. *Nat. Rev. Mol. Cell Biol.* **16**, 258-264, doi:10.1038/nrm3931 (2015).

93 Barnes, C. E., English, D. M. & Cowley, S. M. Acetylation & Co: an expanding repertoire of histone acylations regulates chromatin and transcription. *Essays Biochem.* **63**, 97-107, doi:10.1042/EBC20180061 (2019).

94 Hirschey, M. D. & Zhao, Y. Metabolic Regulation by Lysine Malonylation, Succinylation, and Glutarylation. *Mol. Cell. Proteomics* **14**, 2308-2315, doi:10.1074/mcp.R114.046664 (2015).

95 Lin, H., Su, X. & He, B. Protein lysine acylation and cysteine succination by intermediates of energy metabolism. *ACS Chem. Biol.* **7**, 947-960, doi:10.1021/cb3001793 (2012).

96 Bos, J. & Muir, T. W. A Chemical Probe for Protein Crotonylation. *J. Am. Chem. Soc.* **140**, 4757-4760, doi:10.1021/jacs.7b13141 (2018).

97 He, M., Han, Z., Liu, L. & Zheng, Y. G. Chemical Biology Approaches for Investigating the Functions of Lysine Acetyltransferases. *Angew. Chem.* **57**, 1162-1184, doi:10.1002/anie.201704745 (2018).

98 Marmorstein, R. & Zhou, M. M. Writers and readers of histone acetylation: structure, mechanism, and inhibition. *Cold Spring Harb. Perspect. Biol.* **6**, a018762, doi:10.1101/cshperspect.a018762 (2014).

99 Bheda, P., Jing, H., Wolberger, C. & Lin, H. The Substrate Specificity of Sirtuins. *Annu. Rev. Biochem.* **85**, 405-429, doi:10.1146/annurev-biochem-060815-014537 (2016).

100 Schneider, A. *et al.* Acetyltransferases (HATs) as Targets for Neurological Therapeutics. *Neurotherapeutics* **10**, 568-588, doi:10.1007/s13311-013-0204-7 (2013).

101 Di Cerbo, V. & Schneider, R. Cancers with wrong HATs: the impact of acetylation. *Brief. Funct. Genomics* **12**, 231-243, doi:10.1093/bfgp/els065 (2013).

102 Mohammad, H. P., Barbash, O. & Creasy, C. L. Targeting epigenetic modifications in cancer therapy: erasing the roadmap to cancer. *Nat. Med.* **25**, 403-418, doi:10.1038/s41591-019-0376-8 (2019).

103 Wu, Z. *et al.* A chemical proteomics approach for global analysis of lysine monomethylome profiling. *Mol. Cell. Proteomics* **14**, 329-339, doi:10.1074/mcp.M114.044255 (2015).

104 Wang, X., Sidoli, S., Garcia, B. A. Application of Mass Spectrometry in Translational Epigenetics. *Epigenetic Technological Applications*, 55-78, doi:10.1016/B978-0-12-801080-8.00004-1 (2015).

105 Kaczmarska, Z. *et al.* Structure of p300 in complex with acyl-CoA variants. *Nat Chem Biol* **13**, 21-29, doi:10.1038/nchembio.2217 (2017).

106 Robinson, W. G., Nagle, R., Bachhawat, B. K., Kupiecki, F. P. & Coon, M. J. Coenzyme-a Thiol Esters of Isobutyric, Methacrylic, and Beta-Hydroxyisobutyric Acids as Intermediates in the Enzymatic Degradation of Valine. *Journal of Biological Chemistry* **224**, 1-11 (1957).

107 Yun, J. W. *et al.* A novel ACAD8 mutation in asymptomatic patients with isobutyryl-CoA dehydrogenase deficiency and a review of the ACAD8 mutation spectrum. *Clin. Genet.* **87**, 196-198, doi:10.1111/cge.12350 (2015).

108 Santra, S., Macdonald, A., Preece, M. A., Olsen, R. K. & Andresen, B. S. Long-term outcome of isobutyryl-CoA dehydrogenase deficiency diagnosed following an episode of ketotic hypoglycaemia. *Mol Genet Metab Rep* **10**, 28-30, doi:10.1016/j.ymgmr.2016.11.005 (2017).

109 Wu, H. *et al.* Structural basis for substrate specificity and catalysis of human histone acetyltransferase 1. *Proc. Natl. Acad. Sci. U. S. A.* **109**, 8925-8930, doi:10.1073/pnas.1114117109 (2012).

110 Gao, T., Yang, C. & Zheng, Y. G. Comparative studies of thiol-sensitive fluorogenic probes for HAT assays. *Anal Bioanal Chem* **405**, 1361-1371, doi:10.1007/s00216-012-6522-5 (2013).

111 Kabsch, W. Xds. *Acta Crystallogr. D Biol. Crystallogr.* **66**, 125-132, doi:10.1107/S0907444909047337 (2010).

112 Winn, M. D. *et al.* Overview of the CCP4 suite and current developments. *Acta Crystallogr. D Biol. Crystallogr.* **67**, 235-242, doi:10.1107/S0907444910045749 (2011).

113 Evans, P. R. & Murshudov, G. N. How good are my data and what is the resolution? *Acta Crystallogr. D Biol. Crystallogr.* **69**, 1204-1214, doi:10.1107/S0907444913000061 (2013).

114 Emsley, P., Lohkamp, B., Scott, W. G. & Cowtan, K. Features and development of Coot. *Acta Crystallogr. D Biol. Crystallogr.* **66**, 486-501, doi:10.1107/S0907444910007493 (2010).

115 Williams, C. J. *et al.* MolProbity: More and better reference data for improved all-atom structure validation. *Protein Sci.* **27**, 293-315, doi:10.1002/pro.3330 (2018).

116 Grevengoed, T. J., Klett, E. L. & Coleman, R. A. Acyl-CoA metabolism and partitioning. *Annu Rev Nutr* **34**, 1-30, doi:10.1146/annurev-nutr-071813-105541 (2014).

117 Abdinejad, A., Fisher, A. M. & Kumar, S. Production and utilization of butyryl-CoA by fatty acid synthetase from mammalian tissues. *Arch Biochem Biophys* **208**, 135-145 (1981).

118 Webster, L. T., Jr., Gerowin, L. D. & Rakita, L. Purification and Characteristics of a Butyryl Coenzyme a Synthetase from Bovine Heart Mitochondria. *J Biol Chem* **240**, 29-33 (1965).

119 Roe, C. R. *et al.* Isolated isobutyryl-CoA dehydrogenase deficiency: an unrecognized defect in human valine metabolism. *Mol. Genet. Metab.* **65**, 264-271, doi:10.1006/mgme.1998.2758 (1998).

120 Han, Z. *et al.* Revealing the protein propionylation activity of the histone acetyltransferase MOF (males absent on the first). *J. Biol. Chem.* **293**, 3410-3420, doi:10.1074/jbc.RA117.000529 (2018).

121 Yang, C. *et al.* Labeling lysine acetyltransferase substrates with engineered enzymes and functionalized cofactor surrogates. *J. Am. Chem. Soc.* **135**, 7791-7794, doi:10.1021/ja311636b (2013).

122 Yang, Y. Y., Ascano, J. M. & Hang, H. C. Bioorthogonal chemical reporters for monitoring protein acetylation. *J. Am. Chem. Soc.* **132**, 3640-3641, doi:10.1021/ja908871t (2010).

123 Pougovkina, O., te Brinke, H., Wanders, R. J. A., Houten, S. M. & de Boer, V. C. J. Aberrant protein acylation is a common observation in inborn errors of acyl-CoA metabolism. *J. Inherit. Metab. Dis.* **37**, 709-714, doi:DOI 10.1007/s10545-014-9684-9 (2014).

124 Henry, R. A., Kuo, Y. M., Bhattacharjee, V., Yen, T. J. & Andrews, A. J. Changing the selectivity of p300 by acetyl-CoA modulation of histone acetylation. *ACS Chem. Biol.* **10**, 146-156, doi:10.1021/cb500726b (2015).

125 Dancy, B. M. & Cole, P. A. Protein lysine acetylation by p300/CBP. *Chem. Rev.* **115**, 2419-2452, doi:10.1021/cr500452k (2015).

126 Verreault, A., Kaufman, P. D., Kobayashi, R. & Stillman, B. Nucleosomal DNA regulates the core-histone-binding subunit of the human Hat1 acetyltransferase. *Curr. Biol.* **8**, 96-108 (1998).

127 Papait, R. *et al.* Genome-wide analysis of histone marks identifying an epigenetic signature of promoters and enhancers underlying cardiac hypertrophy. *Proceedings of the National Academy of Sciences* **110**, 20164, doi:10.1073/pnas.1315155110 (2013).

128 Ran-Ressler, R. R., Bae, S., Lawrence, P., Wang, D. H. & Brenna, J. T. Branched-chain fatty acid content of foods and estimated intake in the USA. *Br. J. Nutr.* **112**, 565-572, doi:10.1017/S0007114514001081 (2014).

129 Jost, M., Born, D. A., Cracan, V., Banerjee, R. & Drennan, C. L. Structural Basis for Substrate Specificity in Adenosylcobalamin-dependent Isobutyryl-CoA Mutase and Related Acyl-CoA Mutases. *J. Biol. Chem.* **290**, 26882-26898, doi:10.1074/jbc.M115.676890 (2015).

130 Carafa, V. *et al.* RIP1-HAT1-SIRT Complex Identification and Targeting in Treatment and Prevention of Cancer. *Clin Cancer Res* **24**, 2886-2900, doi:10.1158/1078-0432.CCR-17-3081 (2018).

131 Chriett, S. *et al.* Prominent action of butyrate over β-hydroxybutyrate as histone deacetylase inhibitor, transcriptional modulator and anti-inflammatory molecule. *Scientific Reports* **9**, 742, doi:10.1038/s41598-018-36941-9 (2019).

132 Louis, P., Hold, G. L. & Flint, H. J. The gut microbiota, bacterial metabolites and colorectal cancer. *Nat. Rev. Microbiol.* **12**, 661-672, doi:10.1038/nrmicro3344 (2014).

133 Parada Venegas, D. *et al.* Short Chain Fatty Acids (SCFAs)-Mediated Gut Epithelial and Immune Regulation and Its Relevance for Inflammatory Bowel Diseases. *Front Immunol* **10**, 277, doi:10.3389/fimmu.2019.00277 (2019).

134 Nguyen, T. V. *et al.* Identification of isobutyryl-CoA dehydrogenase and its deficiency in humans. *Molecular Genetics and Metabolism* **77**, 68-79, doi:https://doi.org/10.1016/S1096-7192(02)00152-X (2002).

135 Santra, S., Macdonald, A., Preece, M. A., Olsen, R. K. & Andresen, B. S. Long-term outcome of isobutyryl-CoA dehydrogenase deficiency diagnosed following an episode of ketotic hypoglycaemia. *Molecular Genetics and Metabolism Reports* **10**, 28-30, doi:https://doi.org/10.1016/j.ymgmr.2016.11.005 (2017).

136 Oglesbee, D. *et al.* Development of a newborn screening follow-up algorithm for the diagnosis of isobutyryl-CoA dehydrogenase deficiency. *Genetics in Medicine* **9**, 108-116, doi:10.1097/GIM.0b013e31802f78d6 (2007).